e-ISSN: 3023-6479

AOR

Volume: 1

Issue: 3

Year: 2024

Archives of Ophtalmological Research

MHA
MEDIHEALTH ACADEMY

Archives of
Ophtalmological Research

Editorial Board

Archives of
Ophtalmological Research

Editorial Board

ENGLISH LANGUAGE EDITOR

STATISTICS EDITOR

DESIGN

Şerife KUTLU
E-mail: mha.editoroffice@gmail.com

Archives of
Ophtalmological Research

Contents

Volume: 1 Issue: 3 Year: 2024

ORIGINAL ARTICLES

REVIEW

CASE REPORTS

Archives of
Ophtalmological Research

Original Article

DOI: 10.51271/AOR-0011

Evaluation of choroidal vascular structure in patients with retinal vein occlusion

Gamze Akyüz Dursun[1], Nurgül Örnek[2]

[1]Department of Ophthalmology, Kırıkkale State Hospital, Kırıkkale, Turkiye
[2]Department of Ophthalmology, Faculty of Medicine, Kırıkkale University, Kırıkkale, Turkiye

Received: 10/05/2024 ◆ Accepted: 19/07/2024 ◆ Published: 26/07/2024

Cite this article: Akyüz Dursun G, Örnek N. Evaluation of choroidal vascular structure in patients with retinal vein occlusion. *Arch Ophthalmol Res.* 2024;1(3):35-39.

Corresponding Author: Gamze Akyüz Dursun, gamzeakyuzz@gmail.com

ABSTRACT

Aims: To evaluate the posterior segment structures and choroidal vascularity of the eye in patients with retinal vein occlusion (RVO) using enhanced depth imaging optical coherence tomography (EDI-OCT).

Methods: Thirty-three treatment-naïve patients with RVO (19 males, 14 females) were examined by EDI-OCT. Subfoveal choroid tickness and choroidal vascularity index (CVI) were used to compare the structural characteristics of the choroid with the eyes of twenty-nine age, and gender-matched controls. EDI-OCT images were binarised using ImageJ program.

Results: Best corrected visual acuity was significantly lower in the affected eyes compared to control group (p=<0.001). Central macular thickness, subfoveal choroidal thickness, choroid stromal area, and total choroid area were found to be significantly higher in the patient group (p=<0.05). CVI was significantly lower in the patient group and no significant difference was found between the groups in terms of intraocular pressure values (p>0.05).

Conclusion: RVO causes significant edema in the choroid stromal area without any change in the choroid lumen area. This structural changes in the choroid evaluated by EDI-OCT, a non-invasive examination, may be used in the diagnosis and follow-up of RVO.

Keywords: Retinal vein occlusion, subfoveal choroid thickness, choroid vascularity index

INTRODUCTION

Retinal vein occlusion (RVO) is the most common retinal vascular disease after diabetic retinopathy.[1] Branch RVO is significantly more common than central RVO, with a fivefold prevalence. The prevalence of RVO in adults is reported at 0.5%.[2,3] Systemic conditions such as hypertension (HT), diabetes mellitus (DM), hyperlipidemia (HL), atherosclerosis and hyperviscosity syndrome play a role in the pathogenesis.[4,5]

The hemodynamics of the choroidal circulation are not fully understood. The role of the choroid, whose main function is to supply nutrients to the outer retinal layers, in the pathogenesis of ocular diseases is well known, but conflicting results have been reported in studies evaluating the choroid and choriocapillaris in RVO.[6-9]

Advances in imaging techniques have allowed us to examine the structural features of the retina and choroid more precisely. In particular, the enhanced depth mode of optical coherence tomography (OCT) allowed us to gain insight into the segmentation and functional status of choroidal layers.

The aim of this study was to investigate the structural changes of the choroid and the choroidal vascularity index in patients with RVO by using the enhanced depth imaging OCT (EDI-OCT).

METHODS

This study was conducted at Kırıkkale University, Faculty of Medicine, Ophthalmology Department according to the principles of the Declaration of Helsinki. EDI-OCT scans were retrieved from the database of the Ophthalmology Department of Kırıkkale University, Faculty of Medicine. Ethical approval for the study was received from the Kırıkkale University Clinical Researches Ethics Committee. (Date: 10.02.2022, Decision No: 03/01). All procedures were carried out in accordance with the ethical rules and the principles of the Declaration of Helsinki.

Subjects

This study was conducted retrospectively. A total of 33 patients (19 males, 14 females) with unilateral central or

branch RVO diagnosed between January 2021 and January 2022 were included in the study. 29 age- and gender-matched volunteers were included as the control group.

Best-corrected visual acuity (BCVA) with Snellen chart, intraocular pressure with pneumotonometer, and EDI-OCT findings (Heidelberg Engineering, Heidelberg, Germany), in which we obtained choroidal measuruments, were recorded.

RVO was diagnosed by OCT and fundus fluorescein angiography (FFA) after detailed history and fundus examination. CRVO was defined as the presence of retinal hemorrhages, a telangiectatic capillary bed, and a dilated venous system in all 4 quadrants. BRVO was defined as the presence of retinal hemorrhages or other biomicroscopic evidence of RVO in less than all four quadrants of the eye. The separate evaluation of occluded and non-occluded areas in patients diagnosed with RVO is schematized in Figure. Ischemic RVO was defined as the presence of >10 nonperfused retinal discs on FFA.

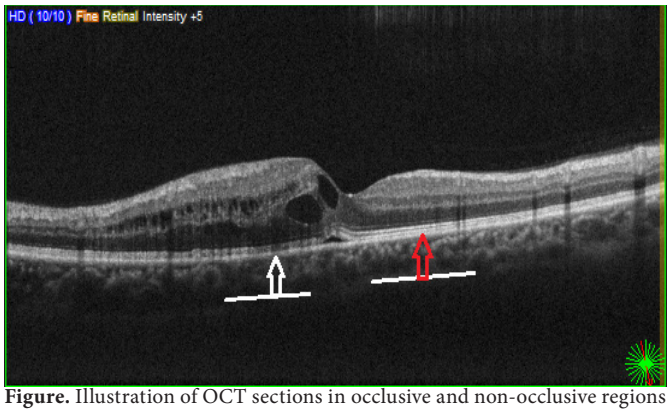

Figure. Illustration of OCT sections in occlusive and non-occlusive regions in patients with branch RVO

OCT: Optical coherence tomography, RVO: Retinal vein occlusion

The exclusion criteria were as follows: refractive errors of more than±six diopters, a history of any ocular trauma, laser treatment, intraocular injections or surgery, and poor-quality OCT images (signal strength index lower than 6 on a 10-point scale) were also excluded.

Measurements

CVI was calculated as the ratio of the area of the lumen (LA) to the total area of the choroid (TCA). For vessel lumen segmentation, the EDI-OCT images were converted to 8-bit format and thresholded using ImageJ (v1.47, NIH). Choroidal binarization followed established methods described in literatüre.[10] Color thresholding was used to further isolate luminal areas from each binarized image. Within a central 1500-µm zone, bright pixels represented the choroidal interstitium and dark pixels represented the vessel lumen.

Statistical Analysis

Statistical analyses were performed with IBM SPSS statistics, version 23.0 (SPSS Inc. Chicago, USA). Descriptive statistics, frequencies and percentages within the groups were reported as (n, %). Before analyzing the relationship between continuous variables between groups, they were subjected to normality analyses considering the number of samples in the groups (Kolmogorov-Smirnov and Shapiro-Wilk tests). Accordingly, variables with normal distribution were reported as mean±standard deviation, and variables with non-normal distribution were reported as median (minimum-maximum). Difference analysis between the two groups in terms of numerical variables was performed using the Student's t test, which compares the means for those with normal distribution, and the Mann-Whitney U test, which compares the median values for those with non-normal distribution. A value of $p<0.05$ was considered statistically significant.

RESULTS

Demographic and clinical characteristics of the groups are shown in Table 1. There was no significant difference between the groups in terms of age and gender (p=0.714, p=0.283 respectively). Body-mass index (BMI) was found to be significantly higher in the patient group than in the control group (p=<0.001).

Table 1. Demographic and clinical features of the groups

	Group 1 (RVO) (n: 33)	Group 2 (Control) (n: 29)	p Value
Age (years)	60.17±9.77	61.90±7.75	0.714¥
Gender (male/female)	19/14	13/16	0.283*
BMI (kg/m²)	32.30±6.09	25.76±3.65	<0.001
Systemic diseases			
None	1		
HT	15		
DM+HT	9		
MTHFR gene mutation	1		
Parkinson' disease	1		
Asthma	1		
HT+CAD	2		
Factor V Leiden MT	3		
Classification of RVO			
Superotemporal RVO	21		
Inferotemporal RVO	8		
Central RVO	4		
Right eye	16		
Left eye	17		
Ischemic RVO	8		
Non-ischemic RVO	25		

RVO: Retinal vein occlusion, BMI: Body-mass index, HT: Hypertension, DM: Diabetes mellitus, MTHFR: Metilentetrahidrofolat redüktaz, CAD: Coronary arter disease, ¥İndependent samples t test, *Chi-square test

The clinical features and OCT findings of the groups are shown in Table 2. BCVA was significantly lower in the affected eyes compared to the control group (p=<0.001). Central macular thickness (CMT), subfoveal choroidal thickness (SCT), stromal area of choroid (SA), and total choroid area (TCA) values were found to be significantly higher in RVO group (p=<0.05). While CVI (LA/TCA ratio) was significantly lower in the RVO group (p=<0.001), LA value was at similar

levels in both groups (p=0.607). No significant difference was found between the groups in terms of IOP values (p>0.05).

Table 2. Comparison of clinical features and OCT findings between groups

	Group 1 (n:33)	Group 2 (Control) (n:29)	p
BCVA (LogMAR)	0.2±0.25	1.00±0.00	<0.001
IOP (mmHg)	15.4±3.8	16.30±2.9	0.845
CMT	560.24±241.50	229.42±15.62	<0.001
SCT	352.45±44.64	277.79±28.29	<0.001
LA	0.38±0.04	0.39±0.06	0.607
SA	0.26±0.03	0.19±0.02	<0.001
TCA	0.64±0.07	0.58±0.08	0.003
CVI	60.80±1.39	68.60±1.37	<0.001

OCT: Optical coherence tomography, BCVA: Best corrected visual acuity, IOP: Intraocular pressure, CMT: Central macular tickness, SCT: Subfoveal choroid tickness, LA: Lumen area, SA: Stromal area, TCA: Total choroid area, CVI: Choroid vascularity index, p: Independent samples t test

Comparison of macular and choroidal thickness values in occlusive and non-occlusive regions in patients with branch RVO occlusion is shown in Table 3. It was observed that both macular and choroidal thickness values were significantly higher in the occlusive group than in the non-occlusive group (p<0.001 for each).

Table 3. Macular and choroidal thicknesses in occlusive and non-occlusive areas in branch RVO eyes

	Group 1	
	Mean±SD	P
Macular tickness, occlusive area (n:23)	640 ±139	<0.001*
Macular tickness, non-occlusive area (n:29)	286 ±17	
Choroid tickness, occlusive area (n:29)	387 ±48	<0.001*
Choroid tickness, non-occlusive area (n:29)	309 ±44	

*Dependent samples t test, RVO:Retinal vein occlusion, SD: Standard deviation

Comparison of macular and choroidal thickness values in the occlusive and non-occlusive regions between the groups is shown in Table 4. Macular and choroidal thicknesses in the occlusive and non-occlusive areas were found to be significantly higher than the control group (p<0.05 for each).

Table 4. Comparison of macula and choroid thicknesses in occlusive and nonocclusive areas with the control group

	Groups		
	Group 1 (RVO) n: 29	Group 2 (Control) n: 29	
	Mean±SD	Mean±SD	P
Macular tickness, Occlusive area	639±137	234±19	<0.001
Macular tickness, Non-occlusive area	292±18	232±12	<0.001
Choroid tickness, Occlusive area	388±48	281±32	<0.001
Choroid tickness, Non-occlusive area	308±42	280±29	0.008

RVO: Retinal vein occlusion, SD: Standard deviation, p: Independent samples t test

DISCUSSION

Choroidal thickness is the most widely used parameter for choroidal assessment but is influenced by many ocular and systemic factors such as age, gender, diurnal variation and ethnicity. Low reproducibility and reliability are the main limitations associated with central choroidal thickness (CCT). Agrawal therefore proposed CVI, a measure of the vascular status of the choroid derived from the ratio of lumen area to total choroidal area.[10] Given that it is less influenced by the aforementioned factors, CVI emerges as a potentially more stable and objective marker for assessing choroidal vascularity. It offers the possibility to ameliorate the limitations of relying solely on CCT measurements. In this paper, CVI was evaluated together with macular and choroidal thickness values in patients with RVO.

It has been shown that the prevalence of RVO increases with age and age is the most important risk factor for RVO.[3] In our study group, the mean age was 61 years, and the most common comorbidity was HT. Among the risk factors identified for RVO, age and HT are the most prominent and their high prevalence in this patient cohort further underscores its prevalence. The rate of ischemic RVO was 24% in our study, which is consistent with the literature.[11-13]

There is a lack of consensus in the evaluation of choroidal thickness in patients with RVO, although many studies have been performed. Tsuiki et al.[14] showed an increase in central choroidal thickness in new cases of RVO in comparison with the contralateral eye. Similarly, there was an increase in choroidal thickness in RVO cases compared to the contralateral eye and a decrease in central choroidal thickness after intravitreal dexamethasone implant treatment.[15,16] In contrast to these results, Du et al.[9] reported that there was no difference in choroidal thickness between eyes with RVO and fellow eyes in their study evaluating chronic RVO cases. In this study, in which we evaluated acute RVO cases, we found that choroidal thickness was higher in eyes with RVO compared with the control group.

Aribas et al.[17] reported that CVI was lower in eyes with RVO compared to healthy eyes and control group. Mitamura et al.[19] reported that eyes with RVO had higher SCT, THA, and SA values in their study using fellow eyes as controls. CVI values were lower, whereas LA values were similar. They also reported that SA and TCA were significantly decreased in the affected eyes 1, 3 and 6 months after intravitreal Avastin administration in RVO cases. Hwang et al.[18] showed that the CVI values were lower in eyes with RVO and macular edema compared to those in healthy eyes. In our study, we found that CVI was lower and SCT, TCA, and SA were higher in eyes with RVO compared to the control group. However, there was no significant difference for LA compared to the control group.

Although RVO is primarily a retinal disease, choroidal changes are likely secondary to retinal pathology. In our report, we found that increased choroidal thickness was due to SA rather than LA enlargement, and that SA enlargement was indicative of choroidal stromal edema. In contrast to other retinal diseases, SA enlargement is remarkable in RVO with macular edema. In a study, only the LA was increased along the choroid in central serous chorioretinopathy,

and both the LA and the SA were increased in diabetic retinopathy.[19] Therefore, the increase in the SA appears to be a specific marker for RVO.

No increase in choroidal thickness was found in eyes with long-term RVO without macular edema. Retinal ischemia induces the production of vascular endothelial growth factor (VEGF), a potent angiogenic factor. In chronic cases without macular edema, intraocular VEGF levels are not thought to be significantly increased.[20] Rayess et al.[21] demonstrated that patients with higher baseline choroidal thickness than healthy eyes had a better response to treatment. This supports the role of excess VEGF in the pathology of choroidal edema in acute cases.

Kim et al.[22] compared eyes with acute RVO with fellow eyes and normal controls and reported that the choroidal thickness in the region of vein occlusion was significantly greater than the choroidal thickness in non-occlusive regions. Localized extravascular fluid leakage and/or high hydrostatic pressure observed in RVO may result from damaged vascular endothelial cells, vasodilation, and increased blood flow through occluded retinal vessels. In our study, we found significantly higher macular and choroidal thicknesses in occluded regions.

Limitations

The small sample size and lack of monitoring of response to treatment can be considered limitations of this study. While our study encompassed both RVO and BRVO patients, investigating these subgroups separately with larger cohorts could yield more definitive answers to specific questions about choroidal alterations in each subtype. In addition, the fact that BMI is not similar between groups reveals BMI bias. However, our study comparing the choroidal findings and choroidal vascular index of newly diagnosed and treatment-naive RVO patients with healthy controls will make a significant contribution to the literature. We think that further studies are needed to see how these parameters will change with treatment in RVO follow-up.

CONCLUSION

The increase in choroidal thickness in eyes with RVO appears to be due to stromal edema, possibly triggered by high intraocular VEGF levels, rather than direct vascular dilatation. These structural changes in the choroid, evaluated by EDI-OCT, a non-invasive examination, can be used in the diagnosis and follow-up of RVO.

ETHICAL DECLARATIONS

Ethics Committee Approval

The study was carried out with the permission of the Kırıkkale University Clinical Researches Ethics Commitee (Date: 10.02.2022, Decision No: 03/01).

Informed Consent

Because the study was designed retrospectively, no written informed consent form was obtained from patients.

Referee Evaluation Process

Externally peer-reviewed.

Conflict of Interest Statement

The authors have no conflicts of interest to declare.

Financial Disclosure

The authors declared that this study has received no financial support.

Author Contributions

All of the authors declare that they have all participated in the design, execution, and analysis of the paper, and that they have approved the final version. All authors certify that they have no affiliations with or involvement in any organization or entity with any financial interest (such as honoraria; educational grants; participation in speakers' bureaus; membership, employment, consultancies, stock ownership, or other equity interest; and expert testimony or patent-licensing arrangements), or non-financial interest (such as personal or professional relationships, affiliations, knowledge or beliefs) in the subject matter or materials discussed in this manuscript.

REFERENCES

1. Rogers S, McIntosh RL, Cheung N, et al. The prevalence of retinal vein occlusion: pooled data from population studies from the United States, Europe, Asia, and Australia. *Ophthalmology* 2010;117:313-319.
2. Klein R, Moss SE, Meuer SM, Klein BE. The 15-year cumulative incidence of retinal vein occlusion: the beaver dam eye study. *Arch Ophthalmol.* 2008;126(4):513-518.
3. Mitchell P, Smith W, Chang A. Prevalence and associations of retinal vein occlusion in Australia. The blue mountains eye study. *Arch Ophthalmol.* 1996;114(10):1243-1247.
4. Dodson PM, Galton DJ, Hamilton AM, Blach RK. Retinal vein occlusion and the prevalence of lipoprotein abnormalities. *Br J Ophthalmol.* 1982;66(3):161-164.
5. Vannas S, Tarkkanen A. Retinal vein occlusion and glaucoma. Tonographic study of the incidence of glaucoma and of its prognostic significance. *Br J Ophthalmol.* 1960;44(10):583-589.
6. Rayess N, Rahimy E, Ying GS, et al. Baseline choroidal thickness as a predictor for treatment outcomes in central retinal vein occlusion. *Am J Ophthalmol.* 2016;171:47-52.
7. Khodabandeh A, Shahraki K, Roohipoor R, et al. Quantitative measurement of vascular density and flow using optical coherence tomography angiography (OCTA) in patients with central retinal vein occlusion: Can OCTA help in distinguishing ischemic from non-ischemic type? *Int J Retina Vitreous.* 2018;27(4):47.
8. Mastropasqua R, Toto L, Di Antonio L, et al. Optical coherence tomography angiography microvascular findings in macular edema due to central and branch retinal vein occlusions. *Sci Rep.* 2017;18(7):40763.
9. Du KF, Xu L, Shao L, et al. Subfoveal choroidal thickness in retinal vein occlusion. *Ophthalmology.* 2013;120(12):2749-2750.
10. Agrawal R, Gupta P, Tan KA, Cheung CM, Wong TY, Cheng CY. Choroidal vascularity index as a measure of vascular status of the choroid: measurements in healthy eyes from a population-based study. *Sci Rep.* 2016; 12;6:21090.
11. Sharma A, D'Amico DJ. Medical and surgical management of central retinal vein occlusion. *Int Ophthalmol Clin.* 2004;44(1):1-16.
12. Grassi P, Naclerio C. Central retinal vein prethrombosis secondary to retinal vasculitis: early detection and treatment. *Middle East Afr J Ophthalmol.* 2020;20;27(2):131-133.
13. Schmidt-Erfurth U, Garcia-Arumi J, Gerendas BS, et al. Guidelines for the management of retinal vein occlusion by the European Society of Retina Specialists (EURETINA). *Ophthalmologica.* 2019;242(3):123-162.
14. Tsuiki E, Suzuma K, Ueki R, Maekawa Y, Kitaoka T. Enhanced depth imaging optical coherence tomography of the choroid in central retinal vein occlusion. *Am J Ophthalmol.* 2013;156(3):543-547.
15. Lee EK, Han JM, Hyon JY, Yu HG. Changes in choroidal thickness after intravitreal dexamethasone implant injection in retinal vein occlusion. *Br J Ophthalmol.* 2015;99(11):1543-1549.

16. Esen E, Sizmaz S, Demircan N. Choroıdal thickness changes after intravitreal dexamethasone implant injection for the treatment of macular edema due to retinal vein occlusion. *Retina.* 2016;36(12):2297-2303.

17. Aribas YK, Hondur AM, Tezel TH. Choroidal vascularity index and choriocapillary changes in retinal vein occlusions. *Graefes Arch Clin Exp Ophthalmol.* 2020;258(11):2389-2397.

18. Hwang BE, Kim M, Park YH. Role of the choroidal vascularity index in branch retinal vein occlusion (BRVO) with macular edema. *PLoS One.* 2021;16(10):e0258728.

19. Kinoshita T, Imaizumi H, Shimizu M, et al. Systemic and ocular determinants of choroidal structures on optical coherence tomography of eyes with diabetes and diabetic retinopathy. *Sci Rep.* 2019;9(1):16228.

20. Noma H, Minamoto A, Funatsu H, et al. Intravitreal levels of vascular endothelial growth factor and interleukin-6 are correlated with macular edema in branch retinal vein occlusion. *Graefes Arch Clin Exp Ophthalmol.* 2006;244(3):309-315.

21. Rayess N, Rahimy E, Ying GS, et al. Baseline choroidal thickness as a short-term predictor of visual acuity improvement following antivascular endothelial growth factor therapy in branch retinal vein occlusion. *Br J Ophthalmol.* 2019;103(1):55-59.

22. Kim KH, Lee DH, Lee JJ, Park SW, Byon IS, Lee JE. Regional choroidal thickness changes in branch retinal vein occlusion with macular edema. *Ophthalmologica.* 2015;234(2):109-18.

Archives of
Ophtalmological Research

Original Article

DOI: 10.51271/AOR-0012

Comparison of axial length, intraocular lens power and refractive results using optical and ultrasound biometry

Ali Ender Kulak[1], Yüksel Totan[2]

[1]Department of Ophthalmology, Sincan Training and Research Hospital, Ankara, Turkiye
[2]Department of Ophthalmology, Private Practice Clinic, Ankara, Turkiye

Received: 20/06/2024 ◆ Accepted: 22/07/2024 ◆ Published: 26/07/2024

Cite this article: Kulak AE, Totan Y. Comparison of axial length, intraocular lens power and refractive results using optical and ultrasound biometry. *Arch Ophthalmol Res*. 2024;1(3):40-45.

Corresponding Author: Ali Ender Kulak, draek50@gmail.com

ABSTRACT

Aims: The aim of the study was to determine whether a new non-contact partial coherence interferometry method utilized by the Nidek-AL Scan agrees sufficiently with applanation ultrasound A-scan technique in intraocular lens power calculation to replace it.

Methods: This was a prospective study of 150 eyes of 125 patients who underwent cataract surgery with the Nidek AL-scan and ultrasound biometry. The intraocular lens power AL and ACD were compared between two methods with Pearson correlation and Bland-Altman analysis. The mean difference between final spherical equivalent refraction and the prediction with each technology was compared.

Results: On average, the axial lengths measured by the Nidek AL-scan were longer by 0.11±0.13 mm compared to the ultrasound biometry ($p<0.001$). Pearson correlation analysis showed a very high correlation between the 2 devices for AL and IOL power ($r>0.90$, $p<0.05$) and a high correlation for ACD (r: 0.886 $p<0.001$). On Bland-Altman analysis, 95% limits of agreement for all parameters were within clinically acceptable limits, and there was good agreement between 2 devices. The mean absolute error when the SRK-T formula for AL-scan was 0.20±0.17 D, whereas for US, 0.29±0.25 D ($p<0.001$).

Conclusion: The intraocular lens power and AL derived from both groups were similar. The agreements between them were high. Two techniques may be used interchangeably.

Keywords: Biometry, axial length, IOL power

INTRODUCTION

Nowadays modern cataract surgery offers refractive surgery as well as visual rehabilitation. It also targets emmetropia. In other words, patients should not wear glasses after surgery. Rapid advances in cataract and refractive surgery, in parallel with these developments, patients vision expectations after surgery have increased. these advantages are cataract surgeries performed through sutureless incisions.[1] widespread use of optical biometrics that take measurements independently of the observer[2] and especially development of aspheric, multifocal and toric intraocular lenses that began to be used.[3] Therefore, it required accurate calculation of intraocular lens power. Refractive errors that occur after cataract surgery cause extreme patient dissatisfaction. Therefore, to calculate consistent and accurate intraocular lens power, the margin of error must be minimal.

Various biometry devices are available today. It works on the principle of 'partial coherence interferometer' IOLMaster (Zeiss) and working with the principle of 'optical low coherence reflectometry' Lenstar (Haag-Streit). AL-scan (Nidek) working with the new 'partial coherence interferometer' method device and is available in our clinic. The most important disadvantage of optical biometrics is that they cannot measure dense cataracts.

It is not able to take measurements or even if it takes measurements, it is taken with low reliability. Zeiss company has developed immersion ultrasound called 'sonolink connection' for IOLMaster. A method that takes measurements using the method and can directly transfer information to optical biometry. NIDEK company also provides A-mode applanation ultrasound measurement for AL-scan. Presented an A-mode ultrasound probe that receives and transmits the same information to AL-scan. Both options presented to solve inability to take measurements in patients with dense cataracts.

The aim of this study is to compare AL-scan optical biometry and which is compactly located in the same device. A-mode ultrasound probe's measurements according to axial length, intraocular lens power and refractive results in terms of consistency and reliability.

METHODS

This prospective sequential cross-sectional non-randomized study was conducted in Turgut Özal University Faculty of Medicine Hospital between August 2013 and March 2014. 150 eyes of 125 patients who underwent phacoemulsification surgery due to cataract were included in the study.

Ethical approval for the study was received from the Turgut Özal University Clinical Researches Ethics Committee (Date: 22.08.2013, Decision No: 825). All procedures were carried out in accordance with the ethical rules and the principles of the Declaration of Helsinki.

Patients who had uncomplicated phacoemulsification surgery and with capsule one-piece hydrophobic acrylic IOL (Tecnis ZCB00, AMO) implantation were included.

Exclusion Criteria

- Optical biometry cannot take axial length measurement
- Previous eye surgery (vitrectomy, excimer laser)
- Patients with visual acuity lower than 20/40 after surgery due to reasons other than cataract (macular degeneration, diabetic macular edema, amblyopia, advanced corneal pathology (dystrophy, existing irregular astigmatism or pterygium)
- Development of complications during surgery (posterior capsule rupture, development of zonule dialysis, placement of a capsule tension ring)
- Corneal astigmatism greater than 2.5 D
- Cataract surgery combined with a secondary procedure (trabeculectomy, limbal relaxing incision)

After a full ophthalmological examination of the cases, all patients are first examined with Nidek AL-scan by an experienced technician. Keratometry, AL, ACD and limbus-limbus distance were measured in automatic dual mode. Then, IOL power was calculated using SRK-T, Hoffer Q, Holladay-1 and Haigis formulas targeting emmetropia postoperatively. Following application of topical anesthetic proparacaine 0.5% (Alcaine 0.5%) drops A-Scan ultrasound mode was switched on and measurements were made with the ultrasound probe as recommended by the company guide. Ten times touched during measurement. Axial lengths taken with ultrasound were transferred to the main screen and IOL power was calculated with SRK-T, Hoffer Q, Holladay-1 and Haigis formula. The power of the IOL to be implanted is SRK-T recommended by optical biometry.

During the surgical procedure, a 2.8 mm wide corneal incision was made, as approximately 5.5 mm diameter capsulorhexis was made, phacoemulsification was performed with WHITESTAR Signature® AMO, and the IOL was placed in the capsular bag. All patients were observed on the 1st day, 1st week and 1st month after surgery. Final refractive results were obtained at 1 month with an autorefractometer (KR 8800, Topcon, Japan) and confirmed by subjective refraction.

Biometry parameters (AL, K, and ACD) and IOL power were compared. To compare the predictability and consistency of biometrics, the target refractive value was compared with the refractive value obtained after surgery. Consistency and predictability were evaluated by numerical error (NE) and absolute error (AE). The difference between the refractive error obtained after the surgery and the target refractive error was determined as 'numerical error' (NE), and the absolute value of the difference between them was determined as 'absolute error' (AE) and evaluated.

Statistical Analysis

The data obtained were recorded on the computer in SPSS 16.0 (statistical Package for the Social Sciences, IBM). Paired samples t test was used to compare the data obtained from the devices. Correlation between measurements was evaluated by Pearson correlation analysis. It is a number between (-1,00 -0,90) and (+1,00 +0,90) values evaluated very good, between (-0,89 -0,70) and (+0,89 +0,70) values evaluted good, between (-0,69 -0,50) and (+0,69 +0,50) values evaluated moderate and between (+0,49 -0,49) values evaluated bad. Evaluations were made within a 95% confidence interval, and a p value of less than 0.05 was considered a statistically significant difference. Bland-Altman plots were drawn to evaluate inter-device agreement. In these graphs, the 95% concordance limit was taken as±1.96 standard deviation.[4]

RESULTS

Patients included in the study 60 were women and 65 were men. The average age of the patients was 63±6.2 years. There was a very good correlation between AL measurements taken with AL-scan and Ultrasound. (r=0.995 p<0.001). There was a good correlation in ACD measurements. (r=0.886 p<0.001). The IOL power obtained with both devices correlates very well according to 4 separate formulas. (r=0.993 for SRK-T, r=0.992 for Hoffer Q, r=0.993 for Holladay, r=0.991 for Haigis).

Mean AL measurements were 23.54±1.33 mm for AL-scan and 23.43±1.35 mm for ultrasound biometry (p<0.001). Higher AL measurements were obtained with AL-scan compared to ultrasound. ACD measurements were 3.17±0.44 mm for AL-scan and 3.16±0.39 mm for ultrasound biometry respectively. (p=0.486). There is a statistically significant difference between the IOL powers obtained by AL-scan and Ultrasound according to 4 formulas (p<0.001). IOL power values obtained with AL-scan are higher than ultrasound biometry (Table 1).

Table 1. Comparison of AL, ACD and IOL power measured by AL-scan and ultrasound biometry

Parameters	AL-scan	A-mode US	p value
AL (mm)	23.54±0.11 (1.33)	23.43±0.11 (1.35)	<0.001
ACD (mm)	3.17±0.035 (0.44)	3.16±0.031 (0.39)	0.486
IOL Power SRK-T (D)	21.06±0.30 (3.76)	20.89±0.30 (3.70)	<0.001
IOL Power Hoffer Q (D)	21.04±0.33 (4.06)	20.77±0.32 (3.97)	<0.001
IOL Power Holladay (D)	21.04±0.32 (3.94)	20.84±0.32 (3.87)	<0.001
IOL Power Haigis (D)	21.09±0.31 (3.82)	20.91±0.32 (3.93)	<0.001

ACD: Anterior chamber depth, IOL: Intraocular optic lens

The mean difference between AL-scan and US was 0.11±0.13 mm for AL and 0.012±0.20 mm for ACD. In terms of IOL power, it was 0.167±0.43 D for SRK-T formula, 0.27±0.50 D for Hoffer Q, 0.20±0.48 D for Holladay, and 0.18±0.53 D for Haigis (Table 2).

Table 2. Difference and compliance range between the parameters measured by AL-scan and ultrasound biometry

		%95 agreement range	
Parameters	**Difference±SD**	**Lower limit**	**Upper limit**
AL (mm)	0.110±0.13	-0.145	0.365
ACD (mm)	0.012±0.20	-0.38	0.40
IOL Power SRK-T (D)	0.167±0.43	-0.69	1.02
IOL Power Hoffer Q (D)	0.27±0.50	-0.72	1.25
IOL Power Holladay (D)	0.20±0.48	-0.75	1.14
IOL Power Haigis (D)	0.18±0.53	-0.86	1.22

SD: Standart deviation, IOL: Intraocular optic lens

When the compatibility of the measurements and IOL power values of both methods was examined with Bland-Altman graphs, the 95% agreement range of all data obtained was narrow and there was good agreement. All data were within clinically acceptable limits (Figure 1).

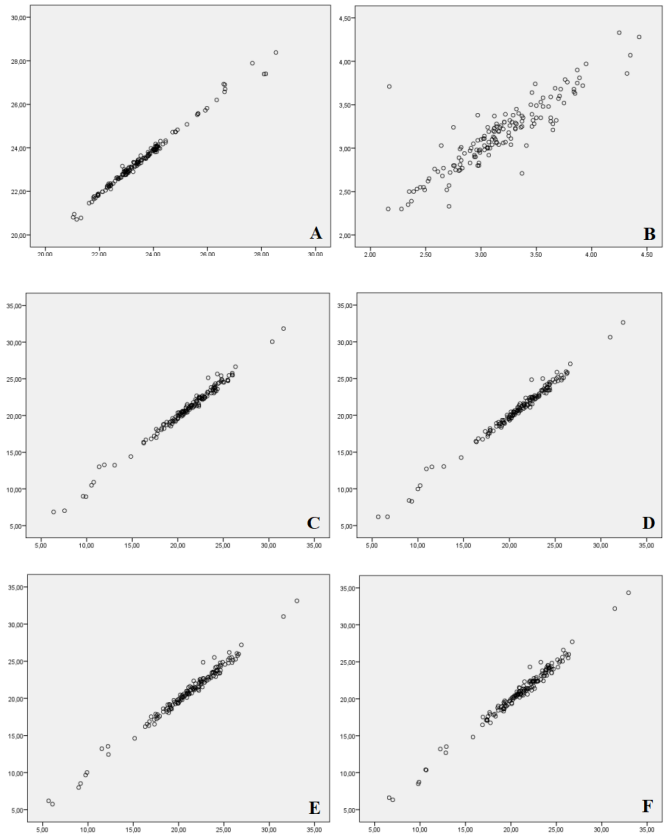

Figure 1. Bland- Altman analysis between AL-scan optical biometry and ultrasound biometry for AL, ACD, A) Axial length, B) Anterior chamber depth, C) IOL power SRK-T, D) IOL power holladay, E) IOL power hoffer Q, F) IOL power haigis
IOL: Intraocular optic lens

While there is no statistically significant difference between the keratometric values obtained from 2.4 mm and 3.3 mm with AL-scan in flat keratometry (K1), there is a significant difference between step keratometry (K2) and average keratometric values (K mean) (p<0.001) (Table 3).

Table 3. Keratometric values

Parameters	**2.4 mm**	**3.3 mm**	**p value**
Flat K, K1 (D)	43.64±1.65	43.62±1.67	0.267
Steep K, K2 (D)	44.47 ±1.71	44.39 ±1.68	<0.001
K Mean (D)	44.05 ±1.65	44.00 ±1.65	<0.001

Considering the refractive results, the average numerical error for AL-scan is -0.02±0.26 D for the SRK-T formula, is -0.01±0.33 D for Hoffer Q, is -0.01±0.28 D for Holladay, is -0.04±0.34 for Haigis respectively. As a for numerical error distrubition 107 eyes (71%) are within±0.25 D, 140 eyes (93%) are within±0.50 D for SRK-T, 84 eyes (56%) are within±0.25 D, 131 eyes (87%) are within±0.50 D for Hoffer Q, 100 eyes (67%) are within±0.25 D, 136 eyes (91%) are within±0.50 D for Holladay, 74 eyes (50%) are within±0.25 D, 128 eyes (85%) are within±0.50 D for Haigis respectively. All eyes are within±1.00 D for all 4 formulas (Table 4, Figure 2).

Table 4. Numerical error and absolute error

	Numerical error			**Absolute error**		
	AL-scan	**Ultrasound**	**p value**	**AL-scan**	**Ultrasound**	**p value**
SRK-T	-0.023±0.26	0.09±0.37	<0.001	0.20±0.17	0.29±0.25	<0.001
Hoffer Q	-0.011±0.33	0.17±0.42	<0.001	0.26±0.21	0.36±0.28	<0.001
Holladay	-0.012±0.28	0.13±0.35	<0.001	0.21±0.19	0.30±0.24	<0.001
Haigis	-0.042±0.34	0.083±0.45	<0.001	0.28±0.20	0.35±0.29	<0.002

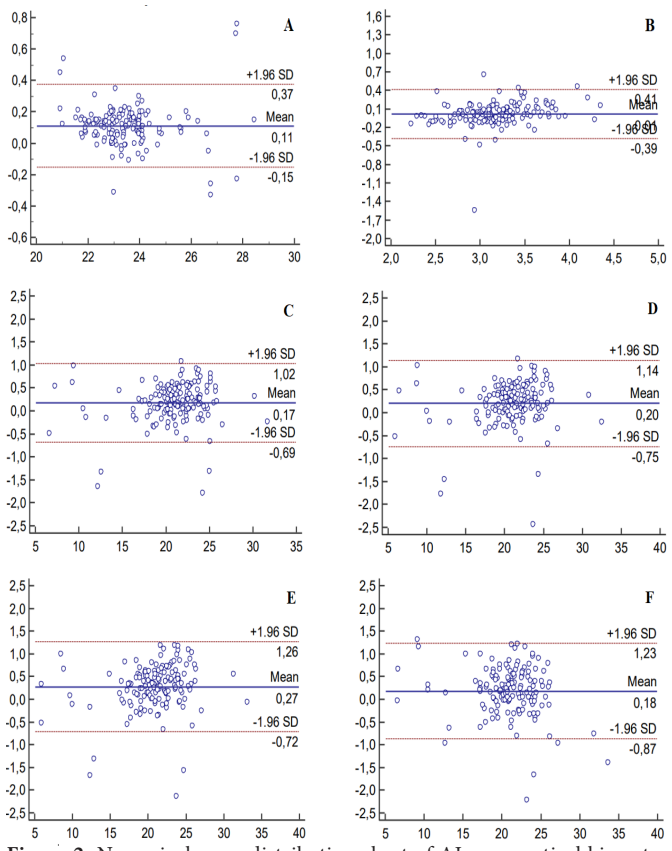

Figure 2. Numerical error distribution chart of AL-scan optical biometry and ultrasound biometry, A) Aksial length, B) Anterior chamber depth, C) IOL power SRK-T, D) IOL power holladay, E) IOL power hoffer Q, F) IOL power haigis
IOL: Intraocular optic lens

The average numerical error for ultrasound biometry is 0.09±0.37 D for the SRK-T formula, is 0.17±0.42 D for Hoffer Q, is 0.13±0.35 D for Holladay, is 0.08±0.45 D for Haigis

respectively. As a for numerical error distrubition 83 eyes (55%) are within ±0.25 D, 124 eyes (83%) are within ±0.50 D for SRK-T, 69 eyes (46%) are within ±0.25 D, 111 eyes (74%) are within ±0.50 D for Hoffer Q, 76 eyes (50%) are within ±0.25 D, 121 eyes (81%) are within ±0.50 D for Holladay, 63 eyes (42%) are within ±0.25 D, 113 eyes (75%) are within ±0.50 D for Haigis respectively. All eyes are within ±1.50 D in the 4 formulas (Table 4, Figure 3).

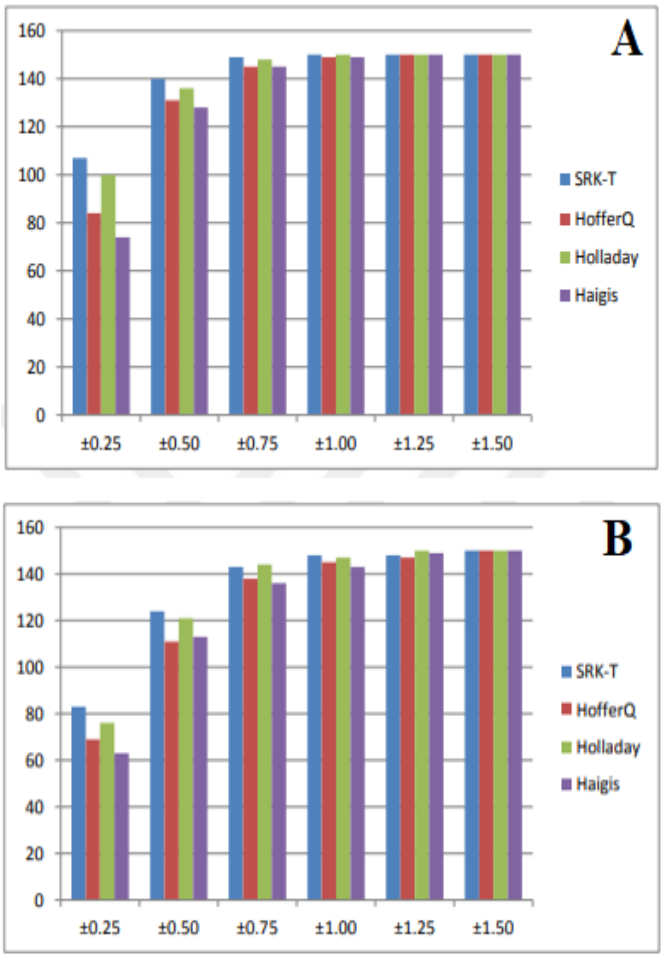

Figure 3. A) Numerical error distrubition chart of AL-scan optical biometer, B) Numerical error distrubition chart of ultrasound biometer

DISCUSSION

When AL cannot be obtained with optical biometrics, many doctors perform IOL power calculating with ultrasound or immersion biometry in addition to auto-keratometry. Keratometry and AL measurements cannot be used interchangeably, even when the efficiency obtained with different biometry methods is used in the same formula. In addition, it is not a practical method to enter an AL measurement that we obtained externally with a different device into the optical biometry device. Due to this structural difficulty, Nidek; In addition to optical biometry, the AL-scan device, which measures axial length with A-mode ultrasound and transfers information to the same device, has been introduced into clinical practice.

In this study, we compared the measurements of AL-scan, a new optical biometry device, with the measurements made by the contact A-mode ultrasound probe in terms of consistency and reliability in terms of axial length, intraocular lens power and refractive results.

Accurate AL measurement is critical in calculating IOL power. Many modifications have been developed for accurate AL measurement with the US method.[5,6] Since the introduction of optical biometrics, accurate measurement of AL has been improved significantly.[7,8] An error of 0.10 mm in AL measurement causes an average refraction deviation of 0.27 D.[8] Additionally, a 1.0 D increase or decrease in IOL power causes a refractive deviation of approximately 0.67 D.[9]

In a study conducted by Eleftheriadis on 100 patients, the average axial length taken with IOLMaster was found to be 0.47 mm longer than the average axial length taken with ultrasonic biometry.[8] In their study comparing Lenstar and US biometry, Buckhurst et al.[10] found the measurements taken from US to be 0.14 mm shorter. In another study by Roncevic et al.,[11] the axial length taken with Lenstar was found to be 0.24±0.25 mm longer than US. Additionally, they found the 95% concordance limit to be between -0.51 and 0.02. Roncevic et al. attributed the applanation US method's ability to obtain shorter AL measurements compared to optical biometry to the pressure on the cornea and the fact that the two methods take measurements from different points. While optical biometrics take measurements from the front surface of the cornea to the retina pigment epithelium, US biometrics take measurements up to the inner limiting membrane. In addition, while optical biometrics take measurements from the visual axis because they are fixation-based, US biometrics take measurements from the optical axis.

In our study, AL-scan optical biometry gave longer results than AL measurements taken with US (0.11±0.29 mm). The 95% concordance limit is between -0.145 and 0.365 and is clinically acceptable.

Apart from Axial Length, one of the other important factors for accurate IOL calculation are keratometric measurements and anterior chamber depth. A 0.1 D error in the keratometry value causes approximately 0.1 D refractive error. When calculating IOL power, optical biometry AL-scan uses K values obtained from 2.4 mm, while US uses K values obtained from 3.3 mm. In the study conducted by Huang et al.[12] with AL Scan, they found that the K values taken from 2.4 mm were 0.03 D steeper for flat K, 0.43 D steeper for steep K, and 0.03 D steeper for average K than the K value taken from 3.3 mm.

In our study, 2.4 mm was 0.02 D for flat K, 0.08 D for vertical K, and 0.08 D for vertical K compared to 3.3 mm. The average K was found to be 0.05 D steeper. While there is no statistically significant difference for flat K ($p=0.267$), there is statistically significant difference for steep K and average K. However, this difference is not clinically significant.

Anterior chamber depth is required when using the biometry formulas Haigis, Holladay 2 and Olsen formulas. Using the Haigis formula, a 0.12 mm difference in anterior chamber depth in an eye with an axial length of 23.5 mm and an average keratometry of 44 D causes a deviation of 0.06 D in the target refractive result.[13] When Savini et al.[14] compared the Sirius device, which measures with the Scheimpflug principle, and A-mode US according to the anterior chamber depth, they found the ACD obtained by the Scheimpflug device to be 0.04 mm deeper than that of A-mode US. In our study, ACD showed a good correlation between AL-scan and US, which work on the Scheimpflug principle (r: 0.886 $p<0.001$). ACD measurements were 3.17±0.44 mm for AL-scan

and 3.16±0.39 mm for ultrasound, respectively, and there was no statistically significant difference (p=0.486). The 95% agreement range was -0.27 to 0.51, indicating good clinical agreement.

In the study conducted by Turhan et al.[15] there was high correlation between biometric measurements and IOL power calculations, however the mean differences between the two biometry devices were significant. Another clinical trial Can et al.[16] considering that Lenstar optical biometry is an acceptable biometric device today and that ultrasound biometry gives different measurements in our results, it is concluded that ultrasound biometry cannot be used instead of new generation optical biometrics, even though there is a very good correlation between the two devices.

In our study, although there is a statistical difference between the two devices in terms of parameters, the confidence interval in the Bland Altman model is within the 95 percent confidence interval. Since our study also includes postoperative refractive results in addition to these studies, it does not seem possible to reach a definitive conclusion without evaluating refractive deviations.

When the IOL power values obtained from AL-scan and US biometry are compared according to the 4 formulas, the IOL power values obtained with AL-scan are higher than those obtained from ultrasound biometry and there is a statistically significant difference. However, when examined by Bland-Altman analysis, there was good agreement between the 2 methods according to all 4 formulas and it was at a clinically acceptable level.

When we examine the numerical and absolute refractive errors obtained by the 2 methods, the average numerical error for AL-scan is -0.02±0.26 D for the SRK-T formula, -0.01±0.33 D for Hoffer Q, -0.01±0.28 for Holladay, respectively. For D and Haigis it is -0.04±0.34 D. The numerical error for ultrasound biometry is 0.09±0.37 D for the SRK-T formula, 0.17±0.42 D for Hoffer Q, 0.13±0.35 D for Holladay, and 0.08±0.45 D for Haigis, respectively. Refractive results obtained with US are more hyperopic than those obtained with AL-scan optical biometry. Although there is a statistically significant difference between the mean numerical errors, it is at a clinically acceptable level.

The absolute error for AL-scan is 0.20±0.17 D, 0.26±0.21 D, 0.21±0.19 D and 0.28±0.20 D for SRK-T, Hoffer Q, Holladay and Haigis formulas, respectively. For US, they are 0.29±0.25 D, 0.36±0.28 D, 0.30±0.24 D and 0.35±0.29 D, respectively.

Refractive results obtained with US biometry showed more deviation from the target refraction than AL-scan. Although there is a statistically significant difference between the absolute errors obtained by the 2 methods, this difference is at a clinically acceptable level.

In their study with IOLMaster and US, Roy et al.[17] obtained absolute refractive error as 0.30±0.25 D and 0.94±1.10 D, respectively. US biometry showed greater deviation from target refraction than IOLMaster.

European Cataract and Refractive Surgery Society reported in 2012, biometric measurements in cataract surgery in order to be considered of good quality, at least 87% of the patient group must have a score of ±1.00 D must be within the refractive error margin.[18]

Rajan et al.[19] also compared IOLMaster with US biometry. While the numerical absolute error was 0.52±0.32 D in the IOLMaster group, it was 0.62±0.40 D in the US group, and US biometry deviated more from the target refraction than IOLMaster.

The disadvantages of our study are that we make a separate classification for short normal and long aksial length and whether the 2 biometric measurements differ in these different groups.

CONCLUSION

As a result, AL, ACD and IOL power values obtained by AL-scan (Nidek) optical biometry and ultrasound biometry offered in the same device complex are in good agreement with each other, and measurement differences and refractive errors between methods are clinically negligible. Therefore, AL-scan optical biometry and ultrasound biometry can be used interchangeably in biometric measurements before cataract surgery.

ETHICAL DECLARATIONS

Ethics Committee Approval

The study was carried out with the permission of Ethical Committee of Turgut Özal University (Date: 22.08.2013, Decision No: 825).

Informed Consent

All patients signed and free and informed consent form.

Referee Evaluation Process

Externally peer-reviewed.

Conflict of Interest Statement

The authors have no conflicts of interest to declare.

Financial Disclosure

The authors declared that this study has received no financial support.

Author Contributions

All of the authors declare that they have all participated in the design, execution, and analysis of the paper, and that they have approved the final version.

REFERENCES

1. Kershner RM. Sutureless one-handed intercapsular phacoemulsification. The keyhole technique. *J Cataract Refract Surg.* 1991;17:719-725.
2. Drexler W, Findl O, Menapace R. Partial coherence interferometry: a novel approach to biometry in cataract surgery. *Am J Ophthalmology.* 1998;126(4):524-534.
3. Bellucci R. Multifocal intraocular lenses. *Curr Opin Ophthalmol.* 2005; 16(1):33-37.
4. Bland JM, Altman DG. Statistical methods for assessing agreement between two methods of clinical measurement. *Lancet.* 1986;1(8476): 307-310.
5. Raj PS, Ilango B, Watson A. Measurement of axial length in the calculation of intraocular lens power. *Eye (London).* 1986;12:227-229.

6. Berges O, Puech M, Assouline M, Letenneur L, Gastellu-Etchegorry M. B-mode guided vector A-mode versus A-mode biometry to determine axial length and intraocular lens power. *J Cataract Refract Surg.* 1998; 24:529-535.

7. Sheng H, Bottjer CA, Bullimore MA. Ocular component measurement using the Zeiss IOLMaster. *Optom Vis Sci.* 2004;81:27-34.

8. Eleftheriadis H. IOLMaster biometry: refractive results of 100 consecutive cases. *Br J Ophthalmolgy.* 2003;87:960-963.

9. Olsen T. Calculation of intraocular lens power: a review. *Acta Ophthalmol.* 2007;85:472-485.

10. Buckhurst PJ, Wolffsohn JS, Shah S, Naroo SA, Davies LN, Berrow EJ. A new optical low coherence reflectometry device for ocular biometry in cataract patients. *British J Ophthalmol.* 2009;93(7):949-953.

11. Roncevic MB, Busic M, Cima I. Comparison of optical low-coherence reflectometry and applanation ultrasound biometry on intraocular lens power calculation *Graefes Arch Clin Exp Ophthalmol.* 2011;249:69-75.

12. Huang J, Savini G. Evaluation of a new optical biometry device for measurements of ocular components and its comparison with IOLMaster. *British J Ophthalmol.* 2014;98(9):1277-1281.

13. Patel R, Pandit R. Comparison of anterior chamber depth measurements from the Galiei dual scheimplug analyzer with IOLMaster. *J Ophthalmol.* 2012;2012:430249.

14. Savini G, Hoffer KJ. Anterior chamber and aqueous depth measurement in pseudophakic eyes: agreement between ultrasound biometry and scheimpflug imaging. *J Refract Surgery.* 2013;29(2):121-125.

15. Akkaya Turhan S, Toker E. Comparison of immersion ultrasound biometry and optical LowCoherence reflectometry for intraocular lens power calculation. *Turk J Clin Experiment Ophtalmol.* 2012;7:219-223.

16. Can E, Duran M. comparison of measurements with optical low coherence reflectometry and contact ultrasound biometry. *J Glaucoma-Cataract.* 2015;10:33-36.

17. Roy A, Das S, Sahu SK, Rath S. Ultrasound biometry vs. IOL Master. *Ophthalmology.* 2012;119(9):1937.e1-1937.e19372. doi:10.1016/j.ophtha.2012.06.006

18. Lundström M, Barry P, Henry Y, Rosen P, Stenevi U. Evidence-based guidelines for cataract surgery: guidelines based on data in the European Registry of Quality Outcomes for Cataract and Refractive Surgery database. *J Cataract Refract Surg.* 2012;38(6):1086-1093.

19. Rajan MS, Keilhorn I, Bell JA. Partial coherence laser interferometry vs conventional ultrasound biometry in intraocular lens power calculations. *Eye (Lond).* 2002;16(5):552-556.

Archives of
Ophtalmological Research

Review

DOI: 10.51271/AOR-0013

Current diagnosis and screening of hydroxychloroquine retinopathy

Hüseyin Egemen Köse, Mehmet Çıtırık

Department of Ophthalmology, Ankara Etlik City Hospital, Ankara, Turkiye

Received: 05/05/2024 ◆ **Accepted**: 12/07/2024 ◆ **Published**: 26/07/2024

Cite this article: Köse HE, Çıtırık M. Current diagnosis and screening of hydroxychloroquine retinopathy. *Arch Ophthalmol Res*. 2024;1(3):46-49.

Corresponding Author: Hüseyin Egemen Köse, egekose1996@gmail.com

ABSTRACT

Hydroxychloroquine-associated retinopathy is an important cause of progressive visual loss that is increasingly being diagnosed with the growing use of hydroxychloroquine and modern imaging techniques. Hydroxychloroquine acts through complex mechanisms and is commonly used to treat rheumatological and dermatological diseases. Optical coherence tomography, fundus autofluorescence, and automated perimetry are commonly used in retinal clinics for the diagnosis and monitoring of hydroxychloroquine-associated retinopathy. Owing to the potential for irreversible central visual loss with the development of retinopathy, early detection of toxicity is crucial. Advances in technology, wide-field imaging devices, new optical coherence tomography techniques and parameters, fundus autofluorescence techniques, and imaging methods such as optical coherence tomography angiography offer promise for the early detection of toxicity.

Keywords: Hydroxychloroquine retinopathy, microperimetry, multifocal electroretinography, optical coherence tomography, optical coherence tomography angiography, perimetry, wide-field imaging

INTRODUCTION

Hydroxychloroquine (HCQ)-associated retinopathy was first described in the 1960s.[1] Hydroxychloroquine is an antimalarial drug that acts through complex mechanisms as an anti-inflammatory, immunomodulatory, anti-infective, and antithrombotic agent. It is commonly used in many rheumatological diseases due to its low cost and efficacy.[2] Additionally, it has been shown to increase survival in patients with systemic lupus erythematosus (SLE).[3] Hydroxychloroquine is a lipophilic and lysosomotropic drug that accumulates in lysosomes within cells, causing lysosomal instability.[4] Hydroxychloroquine retinopathy poses a threat of blindness by causing progressive visual loss, and toxicity can continue to cause damage even after discontinuation of the drug due to accumulation of hydroxychloroquine in the retinal pigment epithelium melanin.[5,6] The term "bull's eye maculopathy," which was traditionally used to describe the end-stage manifestation characterized by parafoveal pigment epithelial changes, has been replaced by the early detection of outer retinal damage without fundoscopic changes following optical coherence tomography (OCT). Therefore, the early detection of this toxicity is important in ophthalmological practice.

PREVALENCE AND RISK FACTORS

Before the widespread use of OCT and fundus autofluorescence (FAF), the prevalence was thought to be less than 0.5%.[7] However, with the increasing use of OCT and FAF, a prevalence of 7.5% in patients using hydroxychloroquine for more than five years and 20-50% in those using it for more than 20 years has been reported. The dose used in the development of retinal toxicity is the most important factor, with the highest risk of toxicity observed at doses >5 mg/kg/day. It has been suggested that the risk is less than 2% with doses of 4-5 mg/kg/day for less than ten years.[8] Another risk factor is the presence of concomitant renal disease. Current evidence suggests that stage 3 (glomerular filtration rate <60 ml/min/1.73 m^2) and worse renal disease pose additional risk. It has also been found that concomitant use of tamoxifen increases the risk.[8] Since patients using hydroxychloroquine for rheumatological diseases are usually older, and concomitant retinal diseases are possible, which are important for both the differential diagnosis of hydroxychloroquine retinopathy and the resulting visual loss. Currently, there is insufficient evidence that preexisting retinal diseases pose an additional risk for hydroxychloroquine retinopathy. However, the detection

of previous retinal diseases is important for the differential diagnosis of hydroxychloroquine retinopathy.[9] Genetic factors have been suggested to play a role in the development of the disease. In a study using exosome sequencing, the RP1L1, RPGR, RPE65, and CCDC66 genes were associated with the onset of the disease.[10] A recent study in patients with SLE also suggests that the use of selective serotonin reuptake inhibitors (SSRIs), selective serotonin-norepinephrine reuptake inhibitors (SNRIs), and antiphospholipid syndrome are risk factors for the development of the disease.[11]

HYDROXYCHLOROQUINE RETINOPATHY PATTERNS

These patterns are based on the localization of the affected retinal pigment epithelium-photoreceptor complex in the fundus.

Parafoveal Retinopathy

Defined as defects in the outer retinal layer between 2° and 6°.

Pericentral Retinopathy

Characterized by defects mainly near major retinal vascular arcades rather than parafoveal. A previous study has shown that this type of involvement is common in Asian patients. Additionally, it is noted that patients with this type of involvement are often in more advanced stages, as the defects are detected late on standard tests (OCT and automated perimetry).[12]

Mixed-Type Retinopathy

Characterized by defects in both the parafoveal and pericentral regions.

HYDROXYCHLOROQUINE RETINOPATHY STAGES

HCQ retinopathy can be divided into early, intermediate, and advanced (severe) stages, based on the degree of involvement of the outer retinal layers. In the early stage, defects in the photoreceptor layer are <180°; in the intermediate stage, defects are >180°; and in the advanced stage, combined retinal pigment epithelium defects (mottled hyper-hypoautofluorescence on FAF) are observed.[13] This classification is also important for disease progression. A study found that in early and intermediate stages, outer retinal involvement did not progress for up to 9 years after discontinuation of the drug, while in advanced retinopathy, progression continued for up to 20 years after discontinuation of the drug.[5]

HYDROXYCHLOROQUINE DIAGNOSTIC TESTS

The tests used for the diagnosis of HCQ retinopathy are divided into structural and functional tests.

Functional Tests

Automated perimetry and visual field test: Visual field tests provide information about visual field loss resulting from retinopathy. They are considered subjective tests due to their variable results and dependence on patient compliance.[14] The most common visual field defect is a ring scotoma in intermediate and severe stages, while in early stages, superonasal field defects may be seen, none of these are specific to HCQ retinopathy.[15] The 10-2 test, although commonly used, may miss pericentral defects, which can be detected with the 24-2 and 30-2 tests.[16,17]

Microperimetry: Microperimetry, which combines automated perimetry with real-time fundus photography, can be used to detect functional loss. Its disadvantages are that it is time-consuming and has a long learning curve for patients. Therefore, it has limited use.[16,17]

Electroretinography and multifocal electroretinography: Full-field electroretinography (ERG) is not recommended as a screening tool because widespread photoreceptor damage is usually observed only in severe cases. Multifocal electroretinography (MfERG) is more sensitive than 10-2 visual field test. Unlike full-field ERG.[18] It is an objective test for detecting decreased function due to retinal toxicity, MfERG can detect localized sensitivity changes in the macula, but it is generally expensive and time-consuming. One systematic review suggested that mfERG have the ability to detect HCQ retinopathy more earlier than other tests used in HCQ screening.[19]

Structural Tests

Structural tests can be classified into standard and newly described structural tests. Standard structural tests are easily accessible in routine practice.

Standard structural Tests: These tests mainly include OCT and fundus autofluorescence (FAF). The earliest OCT finding in early retinopathy is the loss of the parafoveal ellipsoid zone.[20-22] In FAF, parafoveal hyperautofluorescence is observed in early stages, while in advanced stages, patchy hypoautofluorescent areas due to RPE loss begin to appear.[23,24] OCT has been found to be more specific than FAF in a study comparing OCT with FAF.[25]

Newly described structural tests and parameters:

- **Newly described OCT techniques and parameters:** Retinal thinning has been detected as a result of hydroxychloroquine use, and can occur in various forms, including parafoveal, perifoveal, mixed, or total macular thinning.[26] Thinning may be more pronounced in any layer of the retina. Thinning of the inner retinal layers may be an early indicator of HCQ toxicity.[27] Outer retinal layer involvement typically occurs in advanced stages. Thinning of the outer nuclear layer has been shown to be associated with HCQ toxicity.[28] Additionally, these parameters examined by OCT can provide insights into progression during follow-up.[29] Studies have shown that thinning occurs not only in retinal layers but also in choroidal layers.[30,31] Because involvement is often parafoveal in Asian patients, wide-field OCT may be useful in detecting these patients.[12,32] En-face OCT is a newly used imaging technique in daily practice that allows visualization of retinal layers in the coronal plane.[33] Studies using en-face OCT have detected HCQ retinopathy, and quantitative measurements of the affected area have been possible with this imaging technique.[34]

- **Newly described FAF techniques and parameters:** Although FAF has long been used in the detection of HCQ retinopathy, new tests based on FAF are being developed. The first is quantitative FAF measurements. Quantitative fundus autofluorescence (FAF) is a imaging method that primarily divides the macular area into segments of 7°-9° and measures the autofluorescence emitted from stimulated photoreceptors using 488 nm light.[35] Increased quantitative FAF signals have been observed in affected eyes, and it has been found that they begin to increase shortly after starting treatment and remain higher years after discontinuation of the drug.[36,37] Near-infrared FAF is another type of FAF that is used. This imaging allows visualization of autofluorescence derived from melanin pigment in the retina.[38] It has been suggested that HCQ retinopathy can be detected without OCT and fundoscopic signs using this imaging technique.[39] Wide-field FAF has been suggested to be useful in Asian patients.[12,32]
- **Newly described optic coherence tomography angiography parameters:** OCTA, which is increasingly used in retinal practice, has been investigated for its usefulness in detecting HCQ retinopathy with various results. A study in 61 patients diagnosed with HCQ retinopathy using MfERG found that decrease in the density of the deep capillary plexus.[40] Another study compared patients with rheumatoid arthritis with a control group and found no difference in vessel densities.[41]

How should imaging methods be used for hydroxychloroquine toxicity, and when?

According to the American Academy of Ophthalmology (AAO) guidelines published in 2011 and 2016, the initial examination was recommended for patients starting hydroxychloroquine, whereas the Royal College of Ophthalmologists (RCO) did not require the first examination. Both guidelines recommend starting annual examinations five years later if the patient has no major risk factors. However, both guidelines recommend starting screening earlier if the patient's dose is >5 mg/kg/day, if tamoxifen is used concomitantly, or if there is concomitant kidney disease (Table). When choosing a test for toxicity screening, AAO suggests that screening can be performed with OCT, FAF, automated perimetry, or mfERG (using wide-field imaging techniques in Asian patients), whereas RCO recommends OCT and FAF (preferably wide-field) as the first step. According to AAO, the presence of subjective findings confirming an objective test is for toxicity diagnosis. According to the RCO, abnormal OCT and FAF findings are diagnostic for toxicity. If a defect is found on OCT or FAF, automated perimetry and mfERG tests should be performed. If retinal toxicity is detected by an ophthalmologist, the rheumatologist or dermatologist should be informed, and the possibility of discontinuing the drug should be discussed because of the risk of central visual loss.[42,43] There is currently no consensus on or documented screening guidelines in our country.

Table. Screening of hydroxychloroquine retinopathy

For AAO	-In patients starting HCQ (hydroxychloroquine) therapy, the initial examination is performed -If there are no major risk factors; --Annual screening is started in the fifth year (OCT, FAF, automated perimetry, MfERG) --In Asian patients, wider field imaging methods --Subjective findings confirming an objective test=toxicity
For RCO	-In patients starting HCQ therapy, the initial examination is not mandatory. If there are no major risk factors; --Annual screening is started in the fifth year. (If possible, with OCT and FAF in wide angle) --Abnormality in OCT and FAF=Toxicity --If abnormality is found in either OCT or FAF; sequentially, automated perimetry and MfERG tests are performed.
Major risk factors:	Dose >5 mg/kg Use of tamoxifen Kidney disease

AAO: American Academy of Ophthalmology, HCO: Hydroxychloroquine, OCT: Optical coherence tomography, FAF: Fundus autofluorescence, MfERG: Multifocal electroretinography, RCO: Royal College of Ophthalmologists

CONCLUSION

HCQ retinopathy is a disease that is encountered more frequently in daily practice due to the increasing use of HCQ, and it is crucial to prevent irreversible vision loss by early detection. Owing to the limitations of commonly used examinations, such as OCT, FAF, and automated perimetry, in detecting early-stage disease, new imaging models for early disease detection are becoming more widespread in retinal clinics. These methods are gradually becoming a part of our daily use and are expected to continue to do so.

REFERENCES

1. Scherbel AL, Mackenzie AH, Nousek JE, Atdjian M. Ocular lesions in rheumatoid arthritis and related disorders with particular reference to retinopathy. A study of 741 patients treated with and without chloroquine drugs. *N Engl J Med.* 1965;273(7):360-366. doi: 10.1056/nejm196508122730704
2. Yates M, Malaiya R, Stack J, Galloway JB. Hydroxychloroquine use: the potential impact of new ocular screening guidelines. *Eye (Lond).* 2018;32(1):161-162. doi: 10.1038/eye.2017.166
3. Alarcón GS, McGwin G, Bertoli AM, et al. Effect of hydroxychloroquine on the survival of patients with systemic lupus erythematosus: data from LUMINA, a multiethnic US cohort (LUMINA L). *Ann Rheum Dis.* 2007;66(9):1168-1172. doi: 10.1136/ard.2006.068676
4. Mindell JA. Lysosomal acidification mechanisms. *Annu Rev Physiol.* 2012;74:69-86. doi: 10.1146/annurev-physiol-012110-142317
5. Pham BH, Marmor MF. Sequential changes in hydroxychloroquine retinopathy up to 20 years after stopping the drug: implications for mild versus severe toxicity. *Retina.* 2019;39(3):492-501. doi: 10.1097/IAE.0000000000002408
6. Schroeder RL, Gerber JP. Chloroquine and hydroxychloroquine binding to melanin: Some possible consequences for pathologies. *Toxicol Rep.* 2014;1:963-968. doi: 10.1016/j.toxrep.2014.10.019
7. Morsman CD, Livesey SJ, Richards IM, Jessop JD, Mills PV. Screening for hydroxychloroquine retinal toxicity: is it necessary? *Eye (Lond).* 1990;4(Pt 4):572-576. doi: 10.1038/eye.1990.79
8. Melles RB, Marmor MF. The risk of toxic retinopathy in patients on long-term hydroxychloroquine therapy. *JAMA Ophthalmol.* 2014;132(12):1453-1460. doi: 10.1001/jamaophthalmol.2014.3459
9. Yusuf IH, Issa PC, Ahn SJ. Hydroxychloroquine-induced retinal toxicity. *Front Pharmacol.* 2023;14. doi: 10.3389/FPHAR.2023.1196783

10. Chiu HI, Cheng HC, Wu CC, et al. Exome sequencing and genome-wide association analyses unveils the genetic predisposition in hydroxychloroquine retinopathy. *Eye (Lond)*. doi: 10.1038/s41433-024-03044-x

11. Trefond L, Lhote R, Mathian A, et al. Identification of new risk factors for hydroxychloroquine and chloroquine retinopathy in systemic lupus erythematosus patients. *Semin Arthritis Rheum*. 2024;66:152417. doi: 10.1016/j.semarthrit.2024.152417

12. Melles RB, Marmor MF. Pericentral retinopathy and racial differences in hydroxychloroquine toxicity. *Ophthalmology*. 2015;122(1):110-116. doi: 10.1016/j.ophtha.2014.07.018

13. Marmor MF. Comparison of screening procedures in hydroxychloroquine toxicity. *Arch Ophthalmol*. 2012;130(4):461-469. doi: 10.1001/archophthalmol.2011.371

14. Marshall E, Robertson M, Kam S, Penwarden A, Riga P, Davies N. Prevalence of hydroxychloroquine retinopathy using 2018 Royal College of Ophthalmologists diagnostic criteria. *Eye (Lond)*. 2021;35(1):343-348. doi: 10.1038/s41433-020-1038-2

15. Anderson C, Blaha GR, Marx JL. Humphrey visual field findings in hydroxychloroquine toxicity. *Eye (Lond)*. 2011;25(12):1535-1545. doi: 10.1038/eye.2011.245

16. Pfau M, Jolly JK, Wu Z, et al. Fundus-controlled perimetry (microperimetry): application as outcome measure in clinical trials. *Prog Retin Eye Res*. 2021;82:100907. doi: 10.1016/j.preteyeres.2020.100907

17. Rohrschneider K, Bültmann S, Springer C. Use of fundus perimetry (microperimetry) to quantify macular sensitivity. *Prog Retin Eye Res*. 2008;27(5):536-548. doi: 10.1016/j.preteyeres.2008.07.003

18. Lai TYY, Ngai JWS, Chan WM, Lam DSC. Visual field and multifocal electroretinography and their correlations in patients on hydroxychloroquine therapy. *Doc Ophthalmol*. 2006;112(3):177-187. doi: 10.1007/s10633-006-9006-0

19. Tsang AC, Ahmadi Pirshahid S, Virgili G, Gottlieb CC, Hamilton J, Coupland SG. Hydroxychloroquine and chloroquine retinopathy: a systematic review evaluating the multifocal electroretinogram as a screening test. *Ophthalmology*. 2015;122(6):1239-1251.e4. doi: 10.1016/j.ophtha.2015.02.011

20. Omri S, Omri B, Savoldelli M, et al. The outer limiting membrane (OLM) revisited: clinical implications. *Clin Ophthalmol*. 2010;4:183-195. doi: 10.2147/opth.s5901

21. Chen E, Brown DM, Benz MS, et al. Spectral domain optical coherence tomography as an effective screening test for hydroxychloroquine retinopathy (the "flying saucer" sign). *Clin Ophthalmol*. 2010;4:1151-1158. doi: 10.2147/OPTH.S14257

22. Rodriguez-Padilla JA, Hedges TR, Monson B, et al. High-speed ultra-high-resolution optical coherence tomography findings in hydroxychloroquine retinopathy. *Arch Ophthalmol*. 2007;125(6):775-780. doi: 10.1001/archopht.125.6.775

23. Kellner S, Weinitz S, Farmand G, Kellner U. Cystoid macular oedema and epiretinal membrane formation during progression of chloroquine retinopathy after drug cessation. *Br J Ophthalmol*. 2014;98(2):200-206. doi: 10.1136/bjophthalmol-2013-303897

24. Kellner U, Renner AB, Tillack H. Fundus autofluorescence and mfERG for early detection of retinal alterations in patients using chloroquine/hydroxychloroquine. *Invest Ophthalmol Vis Sci*. 2006;47(8):3531-3538. doi: 10.1167/iovs.05-1290

25. Cukras C, Huynh N, Vitale S, Wong WT, Ferris FL, Sieving PA. Subjective and objective screening tests for hydroxychloroquine toxicity. *Ophthalmology*. 2015;122(2):356-366. doi: 10.1016/j.ophtha.2014.07.056

26. Kim KE, Ahn SJ, Woo SJ, et al. Use of OCT retinal thickness deviation map for hydroxychloroquine retinopathy screening. *Ophthalmology*. 2021;128(1):110-119. doi: 10.1016/j.ophtha.2020.06.021

27. Gil P, Nunes A, Farinha C, Teixeira D, Pires I, Silva R. Structural and functional characterization of the retinal effects of hydroxychloroquine treatment in healthy eyes. *Ophthalmologica*. 2019;241(4):226-233. doi: 10.1159/000495308

28. Casado A, López-de-Eguileta A, Fonseca S, et al. Outer nuclear layer damage for detection of early retinal toxicity of hydroxychloroquine. *Biomedicines*. 2020;8(3). doi: 10.3390/biomedicines8030054

29. Melles RB, Marmor MF. Rapid macular thinning is an early ındicator of hydroxychloroquine retinal toxicity. *Ophthalmology*. 2022;129(9):1004-1013. doi: 10.1016/j.ophtha.2022.05.002

30. Ahn SJ, Ryu SJ, Joung JY, Lee BR. Choroidal thinning associated with hydroxychloroquine retinopathy. *Am J Ophthalmol*. 2017;183:56-64. doi: 10.1016/j.ajo.2017.08.022

31. Polat OA, Okçu M, Yılmaz M. Hydroxychloroquine treatment alters retinal layers and choroid without apparent toxicity in optical coherence tomography. *Photodiagnosis Photodyn Ther*. 2022;38:102806. doi: 10.1016/j.pdpdt.2022.102806

32. Lee DH, Melles RB, Joe SG, et al. Pericentral hydroxychloroquine retinopathy in Korean patients. *Ophthalmology*. 2015;122(6):1252-1256. doi: 10.1016/j.ophtha.2015.01.014

33. Leitgeb RA. En face optical coherence tomography: a technology review [Invited]. *Biomed Opt Express*. 2019;10(5):2177-2201. doi:10.1364/BOE.10.002177

34. Ahn SJ, Joung J, Lee BR. En face optical coherence tomography ımaging of the photoreceptor layers in hydroxychloroquine retinopathy. *Am J Ophthalmol*. 2019;199:71-81. doi: 10.1016/j.ajo.2018.11.003

35. Greenberg JP, Duncker T, Woods RL, Smith RT, Sparrow JR, Delori FC. Quantitative fundus autofluorescence in healthy eyes. *Invest Ophthalmol Vis Sci*. 2013;54(8):5684-5693. doi: 10.1167/iovs.13-12445

36. Reichel C, Berlin A, Radun V, et al. Quantitative fundus autofluorescence in systemic chloroquine/hydroxychloroquine therapy. *Transl Vis Sci Technol*. 2020;9(9):42. doi: 10.1167/tvst.9.9.42

37. Greenstein VC, Lima de Carvalho JR, Parmann R, et al. Quantitative fundus autofluorescence in HCQ retinopathy. *Invest Ophthalmol Vis Sci*. 2020;61(11):41. doi: 10.1167/iovs.61.11.41

38. Abdolrahimzadeh S, Ciancimino C, Grassi F, Sordi E, Fragiotta S, Scuderi G. Near-infrared reflectance imaging in retinal diseases affecting young patients. *J Ophthalmol*. 2021;2021:5581851. doi: 10.1155/2021/5581851

39. Kellner S, Weinitz S, Kellner U. Spectral domain optical coherence tomography detects early stages of chloroquine retinopathy similar to multifocal electroretinography, fundus autofluorescence and near-infrared autofluorescence. *Br J Ophthalmol*. 2009;93(11):1444-1447. doi: 10.1136/bjo.2008.157198

40. Akhlaghi M, Kianersi F, Radmehr H, Dehghani A, Naderi Beni A, Noorshargh P. Evaluation of optical coherence tomography angiography parameters in patients treated with Hydroxychloroquine. *BMC Ophthalmol*. 2021;21(1):209. doi: 10.1186/s12886-021-01977-5

41. Esser EL, Zimmermann JA, Storp JJ, Eter N, Mihailovic N. Retinal microvascular density analysis in patients with rheumatoid arthritis treated with hydroxychloroquine. *Graefes Arch Clin Exp Ophthalmol*. 2023;261(5):1433-1442. doi: 10.1007/s00417-022-05946-6

42. Marmor MF, Kellner U, Lai TYY, Melles RB, Mieler WF. American Academy of Ophthalmology. Recommendations on screening for chloroquine and hydroxychloroquine retinopathy (2016 Revision). *Ophthalmology*. 2016;123(6):1386-1394. doi: 10.1016/j.ophtha.2016.01.058

43. Yusuf IH, Foot B, Lotery AJ. The Royal College of Ophthalmologists recommendations on monitoring for hydroxychloroquine and chloroquine users in the United Kingdom (2020 revision): executive summary. *Eye (Lond)*. 2021;35(6):1532-1537. doi: 10.1038/s41433-020-01380-2

Archives of
Ophtalmological Research

Case Report

DOI: 10.51271/AOR-0014

Posterior polar annular choroidal dystrophy: a synopsis of choroidal dystrophies impacting the central macula through a case report

Ertuğrul Köylü, Mehmet Çıtırık, Mehmet Yasin Teke

Department of Ophthalmology, Ankara Etlik City Hospital, Ankara, Turkiye

Received: 01/05/2024 ◆ **Accepted**: 08/07/2024 ◆ **Published**: 26/07/2024

Cite this article: Köylü E, Çıtırık M, Teke MY. Posterior polar annular choroidal dystrophy: a synopsis of choroidal dystrophies impacting the central macula through a case report. *Arch Ophthalmol Res*. 2024;1(3):50-52.

Corresponding Author: Ertuğrul Köylü, ertugrulkoylu95@gmail.com

ABSTRACT

Posterior polar annular choroidal dystrophy (PPACD) is an uncommon disease characterized by atrophy of the retinal pigment epithelium and choriocapillaris in an annular pattern. To date, only a limited number of cases has been reported. PPACD is a distinctive form of primary choroidal dystrophy affecting the central macula, and all forms of these dystrophies exhibit distinctive atrophy patterns. Here, we present a case of PPACD and emphasize the importance of this disease group by providing a brief summary of primary choroidal dystrophies affecting the central macula.

Keywords: Central macula, choroidal dystrophies, fluorescein angiography, posterior polar annular choroidal dystrophy

INTRODUCTION

Posterior polar annular choroidal dystrophy (PPACD), a form of primary choroidal dystrophy affecting the central macula, is a rare ocular disease characterized by atrophy of the retinal pigment epithelium (RPE) and choriocapillaris encircling the optic nerve head and retinal vascular arcades.[1] Since Yanuzzi initially described the term PPACD in 2010,[2] only a limited number of cases have been reported because of the rarity of the condition. The objective of this study was to present a case of PPACD and discuss other forms of primary choroidal dystrophies that affect the central macula, with a comparison to our case.

CASE

A 56-year-old female patient who was referred to the retina clinic underwent evaluation. The patient denied acute vision loss and had no significant medical history. There was no family history of hereditary eye disease. Upon visual acuity examination, the patient's best-corrected visual acuity was 20/32 in both eyes. With Goldmann applanation, the intraocular pressure (IOP) was 13 mmHg on the right and 17 mmHg on the left. Facial symmetry, external face, and ocular alignment were normal on examination. The anterior segment slit-lamp examination was unremarkable in both eyes. Dilated fundus examination of each eye revealed chorioretinal atrophy surrounding the optic disc extending along the temporal vascular arcade, forming an annular pattern with preservation of the fovea. Atrophic appearance was more extensive in the left eye than in the right eye. Sporadic pigment clusters were observed in both eyes. No arteriolar attenuation or bone spicule-like pigmentary changes were observed. Examination of the optic nerve head and peripheral fundus revealed no additional pathology (Figure A, B).

Fluorescein angiography showed that large choroidal vessels could be visualised along the vascular arcades in the right eye and around the macula in the left eye in a concentric pattern due to the atrophy of the RPE and the choriocapillaris. Additionally, late-phase staining in the atrophic region surrounding the optic nerve head was observed in both the eyes (Figure C, D). Fundus autofluorescence imaging revealed well-defined hypoautofluorescence in an annular pattern around the fovea and optic disc, corresponding to the regions of chorioretinal atrophy. On the basis of these findings, a diagnosis of PPACD was established.

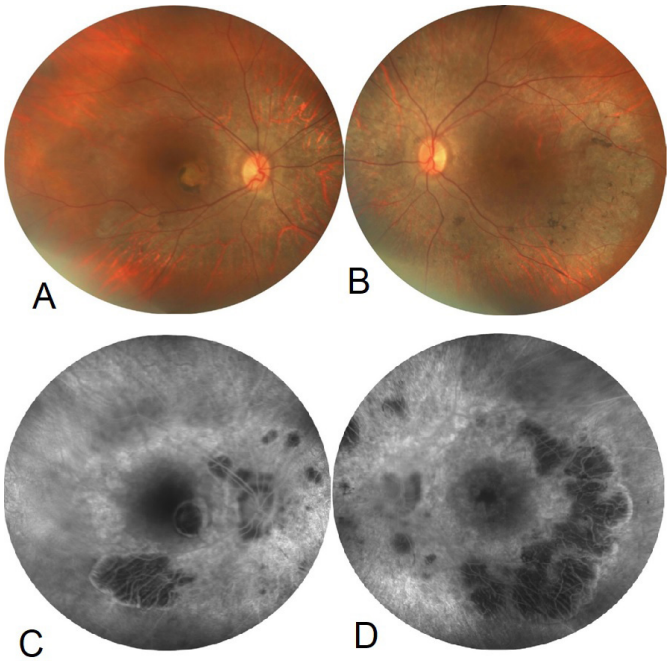

Figure. (A) Color fundus photographs of the right and (B) Left eyes demonstrate bilateral peripapillary atrophy extending along the temporal arcades in an annular pattern. (C) Fluorescein angiography of the right and (D) Left eyes reveals extensive retinal pigment epithelium and choriocapillaris atrophy, allowing the visualization of large choroidal vessels

DISCUSSION

Primary choroidal dystrophies affecting the central macula constitute a discrete group of diseases that exhibit diverse patterns of atrophy, affecting both the retinal pigment epithelium (RPE) and choriocapillaris. The following conditions are considered primary choroidal dystrophies affecting the central macula: central areolar choroidal dystrophy, posterior polar central choroidal dystrophy, posterior polar annular dystrophy, posterior polar hemispheric dystrophy, and central and peripheral annular choroidal dystrophy.[1]

Central areolar choroidal dystrophy (CACD) usually manifests with localized parafoveal pigmentary alterations at the initial stage of the disease, which then progress into a bilateral, symmetrical, atrophic region at the center of the macula.[3] The atrophic region is well-defined and delineated from the surrounding normal retina by distinct borders. With atrophy of the RPE and choriocapillaris, the larger choroidal vessels become apparent. While instances of autosomal recessive transmission have been reported, autosomal dominant inheritance resulting from mutations in the peripherin-2 gene is the prevailing pattern in the majority of cases. Differential diagnosis should be made, especially with atrophic age-related macular degeneration.[3] In contrast to PPACD, there are no areas of atrophy along the vascular arcades or surrounding the optic disc.

In posterior polar central choroidal dystrophy, atrophic anomalies affect the posterior fundus within the vascular arcades and occasionally extend to the region surrounding the optic nerve. Initially, the disease may present as a localized degenerative process, later progressing to involve the entire posterior pole.[4] In PPACD, the fovea is typically preserved, as observed in our case.

In posterior polar hemispheric dystrophy, the atrophic alteration affects half of the posterior pole, extending from the juxtafoveal area to the vascular arcade.[4] In PPACD, a ring-like atrophy is observed along the vascular arcades. With the case report documenting posterior polar annular and hemispheric dystrophy in the same patient, there is a proposition that these two conditions might constitute a single entity.[5]

Central and peripheral annular choroidal dystrophy are distinguished by bilateral symmetrical atrophy at the posterior pole, similar to that observed in central choroidal dystrophy. This is accompanied by a sizable ring-like atrophic region and pigmentary alterations on the peripheral fundus.[4] To date, no abnormalities have been reported in the peripheral fundus in patients with PPACD.[6]

While bilateral involvement was observed in all cases of PPACD, asymmetricity was also a common phenomenon.[1] In our case, the atrophic area was more prevalent in the left eye.

Fluorescein angiography typically reveals a window defect in the atrophic region.[6] However, in a study by Forte et al.,[7] hyperfluorescence was observed in atrophic areas. In contrast, our patient showed diffuse hypofluorescence with large choroidal vessels that were easily visible. This suggests that the choriocapillaris is also extensively affected over time by RPE. Furthermore, Narayanan et al.[5] demonstrated a notable reduction in retinal vasculature in the deep capillary plexus as well as loss of the choriocapillaris in the affected regions. In our case, the presence of diffuse RPE and choriocapillaris atrophy with [l]arge choroidal vessels becoming visible on fluorescein angiography may be indicative of late-stage PPACD. Indeed, it has been reported that the area of atrophy spreads and enlarges insidiously in long term follow-up, and cystoid macular edema and retinal vascularization may develop.[7-9] The utilization of multimodal imaging modalities, including fundus autofluorescence, optical coherence tomography, electroretinogram (ERG) and automated perimetry, is also a valuable approach in the diagnosis of PPACD.[7]

Short-wavelength fundus autofluorescence typically shows peripapillary hypoautofluorescence extending to the vascular arcades in an annular pattern, consistent with the areas of the chorioretinal atrophy. On occasion, a perifoveal hyperautofluorescent border may be observed, which indicates the transition between the healthy and atrophic zones.[6] The hyperautofluorescent border indicates an increase in outer segment phagocytosis and lipofuscin accumulation in RPE. This phenomenon is believed to be the initial stage of atrophy, which will subsequently spread to this region over time.[7]

Two case reports have documented a reduction in amplitude of the scotopic and photopic a-waves and b-waves, as well as a decreased 30Hz flicker response and oscillatory potentials with delayed implicit time in the full-field ERG analysis.[1,5] Sone et al.[8] demonstrated a mild reduction in a-wave amplitudes in scotopic and combined rod-cone responses, as well as a slight decrease in cone and 30-Hz flicker responses. Although the chorioretinal atrophy is confined to the posterior pole in PPACD, the reduction in the amplitude of photopic and scotopic a-wave is remarkable in suggesting diffuse photoreceptor dysfunction. The precise genetic etiology of PPACD remains unclear. However, the presence of diffused depressed responses in the full-field ERG, in conjunction with the clinical presentation and symptoms

such as night blindness, suggests that PPACD may share a similar genetic basis to inherited retinal dystrophies.[6] In contrast to the results reported in the literature, Valle et al.[10] reported a decrease in cone response and a normal rod response in the ERG analysis.

Perimetry showed ring scotoma in two previous reported cases.[5,8] In the case report published by Sone et al.,[8] kinetic perimetry revealed that the ring scotoma was consistent with areas of chorioretinal atrophy and that there was no concentric constriction of the visual field. In a study conducted by Gala et al.,[1] static automated perimetry demonstrated generalized depressed points, particularly in the pericentral area. Furthermore, an enlarged blind spot due to peripapillary atrophy has been documented.[6]

Although no structural or vascular abnormalities can be detected in the fovea with current imaging methods, and the abnormality is mostly around the vascular arcades, the underlying cause of visual acuity loss in patients has not yet been clearly elucidated. A case report by Narayanan et al.[5] demonstrated diffuse functional dysfunction in photoreceptors on the ERG. Another case, as reported by Valle et al.,[10] demonstrated cone dysfunction on ERG. Furthermore, a case study utilising adaptive optics imaging observed the loss of cone photoreceptors in the fovea.[7] When all the evidence is taken together, it may be suggested that the involvement of foveal cone photoreceptors in PPACD cases may result in a deterioration of visual quality or even a decline in visual acuity, as observed in our case. Further investigations are required to elucidate the cause of visual impairment while the fovea remains spared.

CONCLUSION

Primary choroidal dystrophies that affect the central macula constitute a discrete group of diseases that exhibit diverse patterns of chorioretinal atrophy. PPACD is a rare disease that is considered one of the primary choroidal dystrophies affecting the central macula and typically preserves the fovea.

ETHICAL DECLARATIONS

Informed Consent

The patient signed and free and informed consent form.

Referee Evaluation Process

Externally peer-reviewed.

Conflict of Interest Statement

The authors have no conflicts of interest to declare.

Financial Disclosure

The authors declared that this study has received no financial support.

Author Contributions

All of the authors declare that they have all participated in the design, execution, and analysis of the paper, and that they have approved the final version.

REFERENCES

1. Gala JM, Narayanan R. Posterior polar annular choroidal dystrophy. *BMJ Case Rep.* 2019;12(10):e230495.
2. Yannuzzi LA. The Retinal Atlas. Elsevier Health Sciences, Newyork. 2010:80-86.
3. Romano F, Cozzi E, Boon CJF, Staurenghi G, Salvetti AP. Multimodal retinal imaging reveals new pathogenic insights in central areolar choroidal dystrophy: a case series. *Retinal Cases Brief Reports*. 2024; 18(1):32-38.
4. Freund KB, Sarraf D, Mieler WF, Yannuzzi LA. The Retinal Atlas. 2nd ed. Elsevier Health Sciences 2016;204-210.
5. Narayanan R. Posterior polar annular and hemispheric choroidal and retinal dystrophy: optical coherence tomographic angiography description of a rare case. *Indian J Ophthalmol*. 2018;66(12):1874-1876.
6. Ruggeri F, Ciancimino C, Guillot A, et al. Posterior polar annular choroidal dystrophy: Genetic insights and differential diagnosis in inherited retinal diseases. *Curr Issues Mol Biol*. 2024;46(2):1383-1397.
7. Forte R, Aptel F, Feldmann A, Chiquet C. Multimodal imaging of posterior polar annular choroidal dystrophy. *Retin Cases Brief Rep*. 2018;12(1):29-32.
8. Sone R, Noda K, Hirooka K, Saito M, Ishida S. Insidious progression of atrophic lesions in a case of posterior polar annular choroidal dystrophy. *Am J Ophthalmol Case Rep*. 2022;28:101708.
9. Bommakanti N, Besirli CG, Zhao PY. Retinal neovascularization in posterior polar annular choroidal dystrophy. *JAMA Ophthalmol*. 2023; 141(1):102-104.
10. Del Valle-Nava F, Sánchez-Ramos J, Hernández-Vázquez A, Gonzalez-Saldivar G, Ramirez-Estudillo A. Posterior polar annular choroidal dystrophy association with cystoid macular edema. *Clin Case Rep*. 2019;7(2):389-390.

Archives of
Ophtalmological Research

Case Report

DOI: 10.51271/AOR-0015

Delayed-onset infection by atypical pathogens 35 years post-frontalis sling surgery

Nazan Acar Eser[1], Emine Şen[2], Ebru Evren[3]

[1]*Department of Ophthalmology, Ulucanlar Eye Training and Research Hospital, Ankara, Turkiye*
[2]*Department of Ophthalmology, Ankara Etlik City Hospital, Ankara, Turkiye*
[3]*Department of Medical Microbiology, Faculty of Medicine, Ankara University, Ankara, Turkiye*

Received: 23/05/2024 ◆ **Accepted**: 14/07/2024 ◆ **Published**: 26/07/2024

Cite this article: Acar Eser N, Şen E, Evren E. Delayed-onset infection by atypical pathogens 35 years post-frontalis sling surgery. *Arch Ophthalmol Res.* 2024;1(3):53-55.

Corresponding Author: Nazan Acar Eser, drnazanacar7@gmail.com

ABSTRACT

Frontalis sling suspension (FSS) remains a venerable surgical intervention employed in the management of congenital eyelid ptosis, particularly in cases of compromised levator function. Despite its prevalence, the array of complications associated with this procedure is well-explored and meticulously documented. In this report, we delineate the intriguing case of a 57-year-old male patient who underwent FSS three and a half decades prior, only to manifest recurrent preseptal abscess formation at the silicone rod (SR) site a staggering 35 years post-surgery. This instance stands out not only for the unprecedented delay of abscess onset after FSS but also for the novelty of the microbial strains isolated from this anatomical location, previously unexplored in the medical literature.

Keywords: *Citrobacter freundii, Finegoldia magna*, frontalis sling surgery, ptosis, silicon rod

INTRODUCTION

Frontalis sling surgery (FSS), utilizing a silicone rod (SR), is a well-established technique for addressing severe upper eyelid ptosis, particularly in cases where the levator muscle function is poor or absent.[1] This surgical approach leverages the frontalis muscle to elevate the eyelid, thereby compensating for the deficient levator mechanism. The use of a silicone rod offers several advantages, including durability, flexibility, and biocompatibility, making it a preferred material for creating the sling.[1]

This case report aims to detail postoperative considerations associated with the application of silicone rod frontalis sling surgery in patients with significant upper eyelid ptosis. Additionally, it highlights a rare complication, detailing the case of a patient who developed a silicone rod infection 35 years postoperatively, providing insights into the long-term risks and management strategies for such late-onset infections.

CASE

A 57-year-old man with left upper eyelid preseptal cellulitis who had no underlying systemic disease was referred to our oculoplastic clinic. The patient stated that FSS was performed on his left upper eyelid for congenital ptosis 36 years ago. A preseptal abscess was observed at the SR's location, and the skin overlaying it was found to be sensitive by palpation. During ophthalmological examination, no pathological finding was detected on either anterior or posterior segments. Ocular motility was mildly limited in the upper gaze due to the compression of the abscess. The patient stated this was the fourth time in the past twelve months that he had an infection of this kind and had not experienced any infections until last year. To rule out the presence of a systemic disease or condition that could lead to immunosuppression a detailed laboratory workup was performed. Complete blood count, C-reactive protein, erythrocyte sedimentation rate, serological tests including HIV, and fasting blood sugar level with hemoglobin A1C (HbA1c) were evaluated and detected in normal ranges. Also, double-stranded DNA antibody, antinuclear antibody, anti-Ro, anti-La, and anti-Sjögren's-syndrome-related antigen A autoantibodies/anti-Sjögren's-syndrome type B autoantibodies all resulted in negative. During the chest X-ray, no abnormal findings were observed. Systemic antibiotic treatment with ampicillin/sulbactam combination (750 mg, twice a day) and metronidazole (500 mg, once a day) administered with hot compress and topical oxytetracycline hydrochloride ointment for one week. The preseptal cellulitis on the area of SR was significantly improved after 48 hours, however, there was no noticeable decrease in the size of the nodular formation at the end of

the first week (Figure 1). During the physical examination after the antibiotic treatment, the abscess formation was soft, mobile, and had well-demarcated borders. Since the patient had a history of relapses after the cessation of the previous antibiotic treatments, surgical abscess drainage was planned in order to prevent any relapse. During the drainage, an incision was made from the upper eyelid crease, and the orbicular muscle fibers were bluntly dissected to visualize SR. After the dissection, a yellow, fragile tissue covering the SR completely was detected (Figure 2). Although the necrotic tissue overlaying the SR was removed with the greatest care, full extraction of the fibrotic tissue and the SR was not possible due to their stiff attachment to the adjacent tarsal tissue. The removed part of the SR and the necrotic tissue were directly placed in a sterile tube containing 1 ml thioglycolate medium for protection of both aerobic and anaerobic microorganisms. Postoperatively, the patient was treated with amoxicillin and clavulanate, topical chloramphenicol ointment 3% for one week. Swelling and inflammatory signs improved after the treatment. The biopsy resulted in granulation tissue for the necrotic material. *Finegoldia magna (F. magna)* and *Citrobacter freundii (C. freundii)* strains were isolated from the microbiological cultures. During a 6-month follow-up, no recurrence was experienced. Eyelid elevation was achieved spontaneously after the treatment and the margin reflex distance of the upper eyelid was measured approximately 1.5 millimeters (Figure 3).

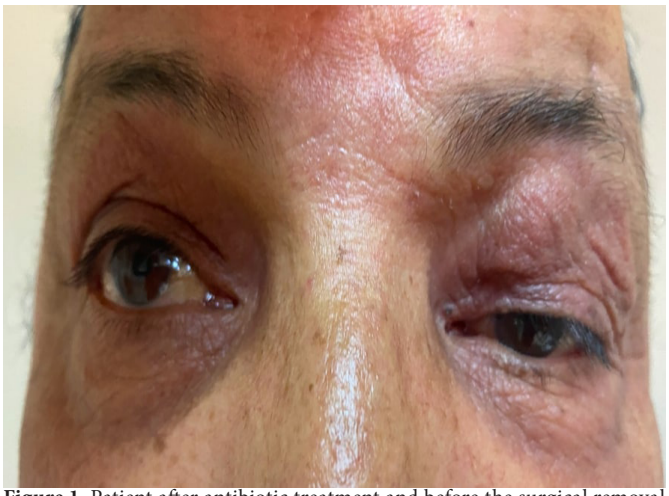

Figure 1. Patient after antibiotic treatment and before the surgical removal of the silicone rod

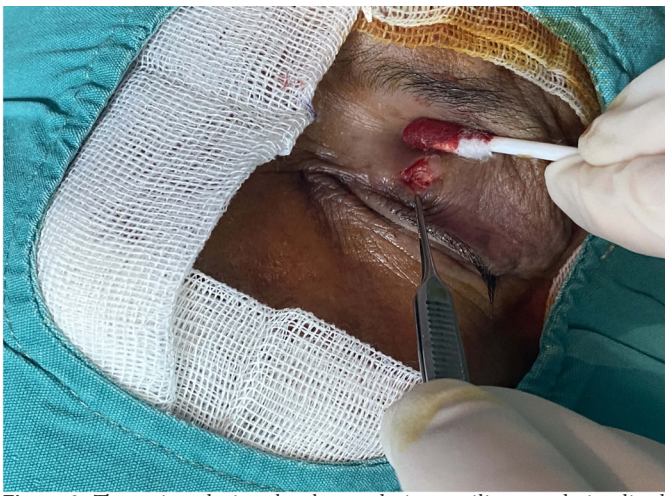

Figure 2. The patient during the abscess drainage, silicone rod visualized and observed covered by a yellow, fragile tissue

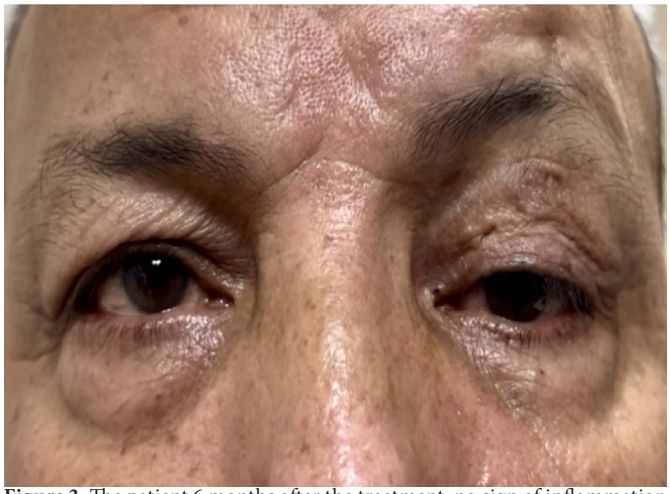

Figure 3. The patient 6 months after the treatment, no sign of inflammation and upper eyelid elevation was observed

DISCUSSION

The current patient presents an unusual case of an FSS resulting in a local inflammatory response with purulent discharge 35 years after a congenital ptosis correction with an SR. This is the first case reported in the literature in which late-onset inflammation was observed for the longest period of time following the FSS. The other published case with a late-onset infection on the surgical site was reported by Hostovsky et al.[2] years after the FSS. In the current case, segmental removal of the necrotic material that overlays the SR adequately managed to cessation of recurrence of the previous infection. The eventual outcome was favorable. Complete SR removal must be taken into account in FSS to prevent problems like infection and extrusion; however, in the present case, it was not possible due to potential tissue damage from the extensive extraction.[3] Our case indicates that it might be beneficial to prevent a localized infection by removing a certain amount of infected tissues.

In the current literature, cases of postoperative wound infections after FSS caused by *nontuberculous mycobacterial* infections are documented.[4] In the current case the isolated strains were in contrast with the literature findings. *F. magna* is an anaerobic, gram-positive *coccus* that rarely causes implant-related infections of bone and joints.[5] It also has been isolated from soft tissue abscesses and acute as well as chronic wound infections.[6,7] *F. magna* is a member of the human gut microbiome and is also frequently found on the skin.[6] It adheres to inert surfaces and has the ability of to produce biofilms but it is responsive to the majority of antibiotics.[6] *F. magna*'s incidence of clinical infections is likely underreported due to difficulty cultivating it and obtaining high-quality anaerobic specimens.[7] About 90% of *F. magna* types possess special enzymes and proteins that facilitate adhesion to specific layers of the skin, enabling it to get through the patient's protective barrier and induce rapid and persistent infections.[8]

Citrobacter species are members of the *Enterobacteriaceae* family of facultative, anaerobic, gram-negative bacilli which are typically detected in water, soil, food, and human intestines.[9] Previously identified as pollutants with low virulence, they are directly linked to a broad range of diseases involving soft tissue.[9,10] *C. freundii* represents an important pathogen, particularly in immunocompromised

people however sporadic infections can occur, and strains could cause wound infections.[9] There is only one case of an immunocompetent patient who developed a spontaneous skin infection caused by *C. freundii*.[10] The isolation of this bacteria is surprising since it has the tendency to infect mostly immunocompromised patients and there is no published case of isolation this strain from periocular area. Since our patient is immunocompetent and the wound infection has been going on for a long time and has not been treated adequately, these could all lead to the reproduction of *C. freundii*. This finding should be supported by other comprehensive studies with materials obtained from other wound infections and abscesses.

The current case stands as an extraordinary rarity, characterized by the unprecedented timing of abscess formation and the isolation of remarkably unusual strains. As far as our extensive exploration into medical literature extends, this case marks the first instance of soft tissue abscess emergence a remarkable 35 years post-FSS. Moreover, the occurrence of a periocular infection attributable to these strains, coupled with such a protracted latency period culminating in abscess formation, remains unparalleled in documented medical records. However, comprehending the mechanism through which these strains induce delayed-onset infections necessitates further comprehensive data gathering. Furthermore, the imperative recognition of these specific strains bears significant importance in the context of late-onset wound infections following surgeries necessitating the use of foreign body implants.

ETHICAL DECLARATIONS

Informed Consent

Written informed consent was obtained from the patient for the publication of this case report and any accompanying images. The patient has reviewed the final draft of the manuscript and consents to its publication. The authors are grateful to the patient for his cooperation and contribution to medical knowledge.

Referee Evaluation Process

Externally peer-reviewed.

Conflict of Interest Statement

The authors have no conflicts of interest to declare.

Financial Disclosure

The authors declared that this study has received no financial support.

Author Contributions

All of the authors declare that they have all participated in the design, execution, and analysis of the paper, and that they have approved the final version.

REFERENCES

1. Chen L, Li J, Zhang C, Li Y, Hou L, Ma J. Surgical interventions for congenital ptosis: a systematic review and meta-analysis of 14 randomized controlled trials. *Aesthetic Plast Surg.* 2023;47(5):1859-1869. doi:10.1007/s00266-023-03360-9
2. Hostovsky A, Waisbourd M, Leibovitch I. Orbital inflammation as a late complication of frontalis silicone elastomer sling operation for congenital ptosis. *J AAPOS.* 2010;14(4):371-372. doi:10.1016/j.jaapos.2010.05.005
3. Bansal RK, Sharma S. Results and complications of silicone frontalis sling surgery for ptosis. *J Pediatr Ophthalmol Strabismus.* 2015;52(2):93-97. doi:10.3928/01913913-20150313-11
4. Walang B, Rath S, Sharma S. Nontuberculous mycobacterial infection after frontalis sling surgery using silicone rod. *J Ophthalmic Inflamm Infect.* 2012;2(4):219-221. doi:10.1007/s12348-012-0073-y
5. Soderquist B, Bjorklund S, Hellmark B, Jensen A, Bruggemann H. *Finegoldia magna* isolated from orthopedic joint implant-associated infections. *J Clin Microbiol.* Nov 2017;55(11):3283-3291. doi:10.1128/JCM.00866-17
6. Donelli G, Vuotto C, Cardines R, Mastrantonio P. Biofilm-growing intestinal anaerobic bacteria. *FEMS Immunol Med Microbiol.* 2012;65(2):318-325. doi:10.1111/j.1574-695X.2012.00962.x
7. Murphy EC, Frick IM. Gram-positive anaerobic cocci-commensals and opportunistic pathogens. *FEMS Microbiol Rev.* 2013;37(4):520-553. doi:10.1111/1574-6976.12005
8. Brinkmann V, Reichard U, Goosmann C, et al. Neutrophil extracellular traps kill bacteria. *Science.* 2004;303(5663):1532-1535. doi:10.1126/science.1092385
9. Lipsky BA, Hook EW, 3rd Smith AA, Plorde JJ. *Citrobacter* infections in humans: experience at the Seattle Veterans Administration Medical Center and a review of the literature. *Rev Infect Dis.* 1980;2(5):746-760. doi:10.1093/clinids/2.5.746
10. Whalen JG, Mully TW, English JC, 3rd. Spontaneous *Citrobacter freundii* infection in an immunocompetent patient. *Arch Dermatol.* 2007;143(1):124-125. doi:10.1001/archderm.143.1.124